

Electronic Supplementary Information
for
**Aluminum complexes containing salicylbenzoxazole ligands
and their application in the ring-opening polymerization of
rac-lactide and ϵ -caprolactone**

Pattarawut Sumrit,[†] Pitak Chuawong,[§] Tanin Nanok,[‡]
Tanwawan Duangthongyou,[‡] Pimpa Homnirun^{*,†}

[†]Laboratory of Catalysts and Advanced Polymer Materials, Department of Chemistry and Center of Excellence for Innovation in Chemistry, Faculty of Science, and [§]Department of Chemistry and Center of Excellence for Innovation in Chemistry, Faculty of Science, and Special Research Unit for Advanced Magnetic Resonance (AMR), and [‡]Department of Chemistry, Faculty of Science, Kasetsart University, Bangkok 10900, Thailand

*E-mail: fscipph@ku.ac.th

Synthesis of 2-hydroxy-3-(1,1-diphenylethyl)-5-methylbenzaldehyde

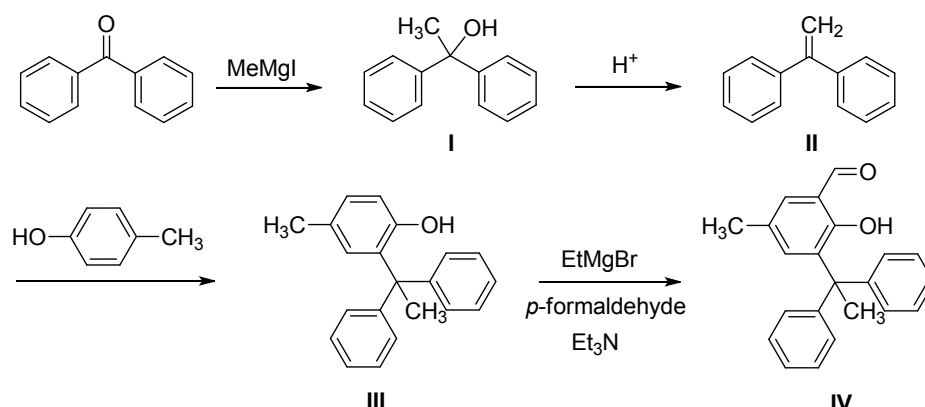


Fig. S1 Synthesis of 2-hydroxy-3-(1,1-diphenylethyl)-5-methylbenzaldehyde.

Synthesis of 1,1-diphenylethanol (I)

To a stirred solution of benzophenone (10.00 g, 54.86 mmol) in diethyl ether (300 mL) was slowly added methylmagnesium iodide (21.95 mL of a 3.0 M solution in diethyl ether, 65.83 mmol) at 0 °C. The reaction mixture was stirred at room temperature for 15 h and a saturated solution of ammonium chloride (50 mL) was then added. The organic phase was separated and the volatiles were removed under reduced pressure to provide a brown solid which was purified by column chromatography (hexane). The product was obtained in 10.12 g (93%).

¹H NMR (500.13 MHz, CDCl₃, 300 K): δ 7.45–7.42 (m, 4H, ArH), 7.36–7.32 (m, 4H, ArH), 7.28–7.24 (m, 2H, ArH), 2.45 (s, 1H, OH), 2.02 (s, 3H, CH₃).

¹³C NMR (125.77 MHz, CDCl₃, 300 K): δ 147.9 (ArC), 128.0 (ArCH), 126.8 (ArCH), 125.8 (ArCH), 76.1 (C), 30.7 (CH₃).

Synthesis of 1,1-diphenylethene (II)

To a stirred solution of 1,1-diphenylethanol (I) (15.00 g, 75.66 mmol) in ethanol (100 mL) was added slowly H₂SO₄ (10.00 mL). The reaction mixture was stirred at room temperature for 24 h. After removal of the volatiles, the product was extracted with dichloromethane. The organic phase was concentrated and purified by column chromatography (hexane). A colorless oil was obtained in 13.00 g (95%).

¹H NMR (500.13 MHz, CDCl₃, 300 K): δ 7.42–7.38 (m, 10H, ArH), 5.53 (s, 2H, CH₂).

¹³C NMR (125.77 MHz, CDCl₃, 300 K): δ 150.0 (C), 141.5 (ArC), 128.2 (ArCH), 128.1 (ArCH), 127.7 (ArCH), 114.2 (CH₂).

Synthesis of 2-(1,1-diphenylethyl)-4-methylphenol (III)

To a stirred solution of 1,1-diphenylethene (**II**) (13.00 g, 72.12 mmol) in toluene (100 mL) was added *p*-cresol (7.80 g, 72.12 mmol) and H₂SO₄ (5.00 mL). The reaction mixture was stirred at room temperature for 24 h. To this reaction, a saturated solution of NaHCO₃ (50 mL) was then added. The organic phase was separated and dried under vacuum to provide a brown oil which was then purified by column chromatography (hexane). The white solid was obtained in 14.00 g (67%).

¹H NMR (500.13 MHz, CDCl₃, 300 K): δ 7.36–7.32 (m, 4H, ArH), 7.29–7.26 (m, 5H, ArH), 7.02 (dd, ³J_{HH} = 8.0 Hz, ⁴J_{HH} = 2.1 Hz, 1H, ArH), 6.76 (d, ⁴J_{HH} = 2.0 Hz, 1H, ArH), 6.76–6.73 (m, 2H, ArH), 4.37 (s, 1H, OH), 2.22 (s, 3H, CH₃), 2.21 (s, 3H, CH₃).

¹³C NMR (125.77 MHz, CDCl₃, 300 K): δ 151.8 (ArC), 146.4 (ArC), 134.1 (ArC), 129.7 (ArCH), 129.6 (ArC), 128.8 (ArCH), 128.5 (ArCH), 128.2 (ArCH), 126.7 (ArCH), 117.8 (ArCH), 51.0 (C), 29.3 (CH₃), 20.8 (CH₃).

Synthesis of 2-hydroxy-3-(1,1-diphenylethyl)-5-methylbenzaldehyde (IV)

To a stirred solution of 2-(1,1-diphenylethyl)-4-methylphenol (**III**) (10.00 g, 34.68 mmol) in THF (100 mL) was slowly added ethylmagnesium bromide (17.34 mL of a 3.0 M solution in diethyl ether, 52.05 mmol) at 0 °C. After the reaction mixture was stirred overnight at room temperature, the volatiles were removed under reduced pressure and then toluene (200 mL) was added. To this solution was then added a mixture of triethylamine (7.24 mL, 52.05 mmol) and paraformaldehyde (2.60 g, 86.70 mmol) in toluene (40 mL). The reaction mixture was stirred at 110 °C for 2 h. Hydrochloric acid (2.0 M, 25 mL) was then added to the reaction mixture. The product was extracted with diethyl ether (3 × 100 mL) and the organic phase was separated. The combined organic phase was dried over MgSO₄, filtered and evaporated under reduced pressure to provide a yellow oil. The crude product was purified by column chromatography (hexane:ethyl acetate = 80:20). The product was obtained as a white solid in 7.07 g (64%).

¹H NMR (500.13 MHz, CDCl₃, 300 K): δ 11.44 (s, 1H, OH), 9.85 (s, 1H, ArCHO), 7.33–7.24 (m, 7H, ArH), 7.17–7.15 (m, 4H, ArH), 6.76 (d, ⁴J_{HH} = 2.2 Hz, 1H, ArH), 2.35 (s, 3H, CH₃), 2.21 (s, 3H, CH₃).

¹³C NMR (125.77 MHz, CDCl₃, 300 K): δ 196.7 (ArCHO), 196.6 (ArC), 158.4 (ArC), 147.6 (ArC), 138.7 (ArCH), 136.9 (ArC), 132.3 (ArCH), 128.2 (ArCH), 127.9 (ArCH), 126.0 (ArCH), 120.6 (ArC), 51.5 (C), 27.4 (CH₃), 20.5 (CH₃).

Synthesis of 2-[(2'-hydroxyphenyl)imino]methylphenol (1)

To a stirred solution of 2-aminophenol (6.00 g, 54.98 mmol) in ethanol (100 mL) was slowly added 2-hydroxybenzaldehyde (6.71 g, 54.98 mmol). Formic acid (2–4 drops) was added as a catalyst. The reaction mixture was then refluxed at 90 °C for 2 h. After cooling to room temperature, red crystals formed. The crystals were collected by filtration and dried under vacuum. Yield: 11.12 g, 95%.

¹H NMR (500.13 MHz, [D₆]DMSO, 300 K): δ 13.82 (br s, 1H, **OH**), 9.75 (br s, 1H, **OH**), 8.97 (s, 1H, **CH=N**), 7.62 (dd, ⁴J_{HH} = 1.5 Hz, ³J_{HH} = 7.8 Hz, 1H, **ArH**), 7.40–7.35 (m, 2H, **ArH**), 7.14 (dt, ⁴J_{HH} = 1.5 Hz, ³J_{HH} = 7.7 Hz, 1H, **ArH**), 6.99 (d, ³J_{HH} = 8.0 Hz, 1H, **ArH**), 6.96–6.94 (m, 2H, **ArH**), 6.89 (dt, ⁴J_{HH} = 1.2 Hz, ³J_{HH} = 7.6 Hz, 1H, **ArH**).

¹³C NMR (125.77 MHz, [D₆]DMSO, 300 K): δ 162.4 (**CH=N**), 161.4 (**ArC**), 151.8 (**ArC**), 135.7 (**ArC**), 133.5 (**ArCH**), 133.0 (**ArCH**), 128.7 (**ArCH**), 120.3 (**ArCH**), 120.2 (**ArC**), 119.4 (**ArCH**), 117.4 (**ArCH**), 117.2 (**ArCH**).

Synthesis of 2,4-dimethyl-6-[(2'-hydroxyphenyl)imino]methyl}phenol (2)

To a stirred solution of 2-aminophenol (5.00 g, 45.82 mmol) in ethanol (100 mL) was slowly added 3,5-dimethyl-2-hydroxybenzaldehyde (6.88 g, 45.82 mmol). Formic acid (2-4 drops) was added as a catalyst. The reaction mixture was then refluxed at 90 °C for 2 h. After cooling to room temperature, red crystals formed. The crystals were collected by filtration and dried under vacuum. Yield: 7.90 g, 71%.

¹H NMR (500.13 MHz, [D₆]DMSO, 300 K): δ 13.90 (s, 1H, **OH**), 9.73 (s, 1H, **OH**), 8.88 (s, 1H, **CH=N**) 7.34 (d, ³J_{HH} = 7.6 Hz, 1H, **ArH**), 7.21 (s, 1H, **ArH**), 7.12 (t, ³J_{HH} = 7.5 Hz, 1H, **ArH**), 7.10 (s, 1H, **ArH**), 6.97 (d, ³J_{HH} = 8.0 Hz, 1H, **ArH**), 6.88 (t, ³J_{HH} = 7.4 Hz, 1H, **ArH**), 2.25 (s, 3H, **CH₃**), 2.19 (s, 3H, **CH₃**).

¹³C NMR (125.77 MHz, [D₆]DMSO, 300 K): δ 162.6 (**CH=N**), 157.6 (**ArC**), 151.8 (**ArC**), 135.7 (**ArC**), 135.3 (**ArCH**), 130.5 (**ArCH**), 128.6 (**ArCH**), 127.3 (**ArC**), 125.6 (**ArC**), 120.3 (**ArCH**), 118.9 (**ArC**), 117.2 (**ArCH**), 20.6 (**CH₃**), 15.9 (**CH₃**).

Synthesis of 2,4-(di-*tert*-butyl)-6-[(2'-hydroxyphenyl)imino]methyl}phenol (3)

To a stirred solution of 2-aminophenol (4.60 g, 42.15 mmol) in ethanol (100 mL) was slowly added 3,5-di-*tert*-butyl-2-hydroxybenzaldehyde (9.87 g, 42.15 mmol). Formic acid (2-4 drops) was added as a catalyst. The reaction mixture was then refluxed at 90 °C for 2 h. After cooling to room temperature, yellow crystals formed. The crystals were collected by filtration and dried under vacuum. Yield: 10.42 g, 95%.

¹H NMR (500.13 MHz, CDCl₃, 300 K): δ 8.71 (s, 1H, **CH=N**), 7.50 (d, ⁴J_{HH} = 2.4 Hz, 1H, **ArH**), 7.27 (d, ⁴J_{HH} = 3.0 Hz, 1H, **ArH**), 7.23–7.19 (m, 1H, **ArH**), 7.16 (dd, ⁴J_{HH} = 1.5 Hz, ³J_{HH} = 7.9 Hz, 1H, **ArH**), 7.03 (dd, ⁴J_{HH} = 1.3 Hz, ³J_{HH} = 8.1 Hz, 1H, **ArH**), 6.98–6.94 (m, 1H, **ArH**), 1.48 (s, 9H, **C(CH₃)₃**), 1.35 (s, 9H, **C(CH₃)₃**).

¹³C NMR (125.77 MHz, CDCl₃, 300 K): δ 165.4 (**CH=N**), 158.0 (**ArC**), 150.1 (**ArC**), 141.5 (**ArC**), 137.4 (**ArC**), 136.3 (**ArC**), 129.0 (**ArCH**), 128.6 (**ArCH**), 127.5 (**ArCH**), 121.2 (**ArCH**), 118.8 (**ArC**), 118.5 (**ArCH**), 118.0 (**ArCH**), 35.4 (**C(CH₃)₃**), 34.5 (**C(CH₃)₃**), 31.7 (**C(CH₃)₃**), 29.7 (**C(CH₃)₃**).

Synthesis of 2,4-dichloro-6- $\{[(2'$ -hydroxyphenyl)imino]methyl}phenol (4)

To a stirred solution of 2-aminophenol (1.70 g, 15.58 mmol) in ethanol (30 mL) was slowly added 3,5-dichloro-2-hydroxybenzaldehyde (2.98 g, 15.58 mmol). Formic acid (2-4 drops) was added as a catalyst. The reaction mixture was then refluxed at 90 °C for 2 h. After cooling to room temperature, red crystals formed. The crystals were collected by filtration and dried under vacuum. Yield: 4.06 g, 92%.

^1H NMR (500.13 MHz, $[\text{D}_6]$ DMSO, 300 K): δ 10.22 (s, 1H, OH), 9.07 (s, 1H, CH=N), 7.65 (d, $^4J_{\text{HH}} = 2.6$ Hz, 1H, ArH), 7.62 (d, $^4J_{\text{HH}} = 2.6$ Hz, 1H, ArH), 7.50 (dd, $^4J_{\text{HH}} = 1.5$ Hz, $^3J_{\text{HH}} = 8.0$ Hz, 1H, ArH), 7.21–7.18 (m, 1H, ArH), 7.01 (dd, $^4J_{\text{HH}} = 1.3$ Hz, $^3J_{\text{HH}} = 8.1$ Hz, 1H, ArH), 6.95–6.91 (m, 1H, ArH).

^{13}C NMR (125.77 MHz, $[\text{D}_6]$ DMSO, 300 K): δ 160.1 (CH=N), 159.5 (ArC), 151.6 (ArC), 132.9 (ArC), 131.9 (ArC), 130.9 (ArCH), 129.8 (ArCH), 123.6 (ArC), 120.7 (ArC), 120.4 (ArCH), 120.1 (ArCH), 119.7 (ArCH), 117.4 (ArCH).

Synthesis of 2,4-dibromo-6- $\{[(2'$ -hydroxyphenyl)imino]methyl}phenol (5)

To a stirred solution of 2-aminophenol (0.78 g, 7.14 mmol) in ethanol (100 mL) was slowly added 3,5-dibromo-2-hydroxybenzaldehyde (2.04 g, 7.14 mmol). Formic acid (2-4 drops) was added as a catalyst. The reaction mixture was then refluxed at 90 °C for 2 h. After cooling to room temperature, red crystals formed. The crystals were collected by filtration and dried under vacuum. Yield: 1.83 g, 90%.

^1H NMR (500.13 MHz, $[\text{D}_6]$ DMSO, 300 K): δ 15.66 (br s, 1H, OH), 10.23 (br s, 1H, OH), 9.06 (s, 1H, CH=N), 7.87–7.84 (m, 1H, ArH), 7.78 (m, 1H, ArH), 7.71 (d, $^3J_{\text{HH}} = 7.6$ Hz, 1H, ArH), 7.20 (t, $^3J_{\text{HH}} = 7.3$ Hz, 1H, ArH), 7.02 (d, $^3J_{\text{HH}} = 8.0$ Hz, 1H, ArH), 6.93 (t, $^3J_{\text{HH}} = 6.0$ Hz, 1H, ArH).

^{13}C NMR (125.77 MHz, $[\text{D}_6]$ DMSO, 300 K): δ 161.6 (CH=N), 159.4 (ArC), 151.6 (ArC), 138.3 (ArCH), 134.7 (ArCH), 131.6 (ArC), 129.8 (ArCH), 120.6 (ArC), 120.4 (ArCH), 119.7 (ArCH), 117.4 (ArCH), 114.2 (ArC), 107.8 (ArC).

Synthesis of 2-isopropyl-6- $\{[(2'$ -hydroxyphenyl)imino]methyl}phenol (6)

To a stirred solution of 2-aminophenol (3.30 g, 30.24 mmol) in ethanol (100 mL) was slowly added 3-isopropyl-2-hydroxybenzaldehyde (5.00 g, 30.24 mmol). Formic acid (2-4 drops) was added as a catalyst. The reaction mixture was then refluxed at 90 °C for 2 h. After the removal of the volatiles, an orange oil was obtained which was then recrystallized from cold hexane. Orange crystals were collected by filtration and dried under vacuum. Yield: 5.30 g, 69%.

^1H NMR (500.13 MHz, CDCl_3 , 300 K): δ 12.59 (br s, 1H, OH), 8.69 (s, 1H, CH=N), 7.38 (d, $^3J_{\text{HH}} = 7.5$ Hz, 1H, ArH), 7.28 (d, $^3J_{\text{HH}} = 7.6$ Hz, 1H, ArH), 7.22 (t, $^3J_{\text{HH}} = 7.6$ Hz, 1H, ArH), 7.15 (d, $^3J_{\text{HH}} = 7.8$ Hz, 1H, ArH), 7.04 (d, $^3J_{\text{HH}} = 8.1$ Hz, 1H, ArH), 6.97 (t, $^3J_{\text{HH}} = 7.6$ Hz, 2H, ArH), 5.83 (br s, 1H, OH), 3.45 (sept, 1H, CH(CH₃)₂), 1.30 (d, $^3J_{\text{HH}} = 6.9$ Hz, 6H, CH(CH₃)₂).

^{13}C NMR (125.77 MHz, CDCl_3 , 300 K): δ 164.6 ($\text{CH}=\text{N}$), 158.3 (ArC), 150.1 (ArC), 136.9 (ArC), 136.1 (ArC), 130.8 (ArCH), 130.6 (ArCH), 128.8 (ArCH), 121.3 (ArCH), 119.6 (ArCH), 118.9 (ArC), 118.5 (ArCH), 116.1 (ArCH), 26.8 ($\text{CH}(\text{CH}_3)_2$), 22.6 ($\text{CH}(\text{CH}_3)_2$).

Synthesis of 2-*tert*-butyl-6- $\{[(2'$ -hydroxyphenyl)imino]methyl}phenol (7)

To a stirred solution of 2-aminophenol (1.20 g, 11.00 mmol) in ethanol (100 mL) was slowly added 3-*tert*-butyl-2-hydroxybenzaldehyde (2.00 g, 11.00 mmol). Formic acid (2-4 drops) was added as a catalyst. The reaction mixture was then refluxed at 90 °C for 2 h. After the removal of the volatiles, a yellow oil was obtained which was then recrystallized from cold hexane. Yellow crystals were collected by filtration and dried under vacuum. Yield: 2.17 g, 72%.

^1H NMR (500.13 MHz, CDCl_3 , 300 K): δ 12.94 (br s, 1H, OH), 8.71 (s, 1H, $\text{CH}=\text{N}$), 7.49 (d, $^3J_{\text{HH}} = 7.4$ Hz, 1H, ArH), 7.33 (d, $^3J_{\text{HH}} = 7.4$ Hz, 1H, ArH), 7.26 (t, $^3J_{\text{HH}} = 7.5$ Hz, 1H, ArH), 7.18 (d, $^3J_{\text{HH}} = 7.6$ Hz, 1H, ArH), 7.09 (d, $^3J_{\text{HH}} = 7.8$ Hz, 1H, ArH), 7.02 (t, $^3J_{\text{HH}} = 7.3$ Hz, 1H, ArH), 6.98 (t, $^3J_{\text{HH}} = 7.7$ Hz, 1H, ArH), 1.54 (s, 9H, $(\text{CH}_3)_3$).

^{13}C NMR (125.77 MHz, CDCl_3 , 300 K): δ 164.9 ($\text{CH}=\text{N}$), 160.3 (ArC), 150.1 (ArC), 138.0 (ArC), 136.0 (ArC), 131.4 (ArCH), 131.3 (ArCH), 128.8 (ArCH), 121.3 (ArCH), 119.5 (ArC), 119.2 (ArCH), 118.6 (ArCH), 116.1 (ArCH), 35.2 ($\text{C}(\text{CH}_3)_3$), 29.6 ($\text{C}(\text{CH}_3)_3$).

Synthesis of 2-phenyl-6- $\{[(2'$ -hydroxyphenyl)imino]methyl}phenol (8)

To a stirred solution of 2-aminophenol (2.75 g, 25.20 mmol) in ethanol (100 mL) was slowly added 3-phenyl-2-hydroxybenzaldehyde (5.00 g, 25.20 mmol). Formic acid (2-4 drops) was added as a catalyst. The reaction mixture was then refluxed at 90 °C for 2 h. After cooling to room temperature, red crystals formed. The crystals were collected by filtration and dried under vacuum. Yield: 6.20 g, 85%.

^1H NMR (500.13 MHz, CDCl_3 , 300 K): δ 13.01 (s, 1H, OH), 8.75 (s, 1H, $\text{CH}=\text{N}$), 7.67–7.65 (m, 2H, ArH), 7.51 (dd, $^4J_{\text{HH}} = 1.7$ Hz, $^3J_{\text{HH}} = 7.5$ Hz, 1H, ArH), 7.50–7.46 (m, 2H, ArH), 7.44 (dd, $^4J_{\text{HH}} = 1.7$ Hz, $^3J_{\text{HH}} = 7.7$ Hz, 1H, ArH), 7.40–7.37 (m, 1H, ArH), 7.23–7.18 (m, 2H, ArH), 7.07 (t, $^3J_{\text{HH}} = 7.6$ Hz, 1H, ArH), 6.99–6.96 (m, 2H, ArH).

^{13}C NMR (125.77 MHz, CDCl_3 , 300 K): δ 163.9 ($\text{CH}=\text{N}$), 159.3 (ArC), 150.2 (ArC), 137.5 (ArC), 135.6 (ArC), 134.9 (ArCH), 132.4 (ArCH), 130.5 (ArC), 129.6 (ArCH), 129.1 (ArCH), 128.5 (ArCH), 127.7 (ArCH), 121.3 (ArCH), 119.8 (ArCH), 119.7 (ArC), 118.4 (ArCH), 116.3 (ArCH).

Synthesis of 2-(1,1-diphenylethyl)-4-methyl-6- $\{[(2'$ -hydroxyphenyl)imino]methyl}phenol (9)

To a stirred solution of 2-aminophenol (1.72 g, 15.80 mmol) in ethanol (100 mL) was slowly added 3-(1,1-diphenylethyl)-5-methyl-2-hydroxybenzaldehyde (5.00 g, 15.80 mmol). Formic acid (2-4 drops) was added as a catalyst. The reaction mixture was then refluxed at 90 °C for 2 h. After cooling to room temperature, red crystals formed. The crystals were collected by filtration and dried under vacuum. Yield: 5.00 g, 78%.

^1H NMR (500.13 MHz, CDCl_3 , 300 K): δ 12.43 (br s, 1H, **OH**), 8.64 (s, 1H, **CH=N**), 7.33–7.29 (m, 4H, **ArH**), 7.26–7.25 (m, 1H, **ArH**), 7.24 (t, $^4J_{\text{HH}} = 2.3$ Hz, 1H, **ArH**), 7.22–7.13 (m, 5H, **ArH**), 7.16–7.15 (m, 1H, **ArH**), 7.10 (dd, $^4J_{\text{HH}} = 1.5$ Hz, $^3J_{\text{HH}} = 7.9$ Hz, 1H, **ArH**), 6.98 (dd, $^4J_{\text{HH}} = 1.3$ Hz, $^3J_{\text{HH}} = 8.1$ Hz, 1H, **ArH**), 6.96–6.92 (m, 1H **ArH**), 6.64–6.63 (m, 1H, **ArH**), 5.70 (br s, 1H, **OH**), 2.39 (s, 3H, **CH₃**), 2.20 (s, 3H, **CH₃**).

^{13}C NMR (125.77 MHz, CDCl_3 , 300 K): δ 164.5 (**CH=N**), 157.5 (**ArC**), 150.2 (**ArC**), 148.4 (**ArCH**), 136.7 (**ArC**), 136.1 (**ArC**), 136.0 (**ArCH**), 132.0 (**ArCH**), 128.8 (**ArCH**), 128.7 (**ArCH**), 128.2 (**ArCH**), 127.8 (**ArC**), 126.2 (**ArCH**), 121.2 (**ArCH**), 119.5 (**ArC**), 118.6 (**ArC**), 116.2 (**ArCH**), 52.1 (**C**), 27.9 (**CH₃**), 21.0 (**CH₃**).

Synthesis of L^3_2AlOBn (**10**)

To a stirred solution of **3b** (0.17 g, 0.25 mmol) in hexane (5 mL) was added one equivalent of benzyl alcohol (26 μL , 0.25 mmol). The reaction mixture was stirred at 40 °C for 5 hours during which the time white solids precipitated. The solids were collected by filtration and dried under vacuum. Yield: 0.15 g, 79%.

^1H NMR (500.13 MHz, toluene- d_8 , 343 K): δ 8.11–8.09 (m, 2H, **ArH**), 8.07 (d, $^4J_{\text{HH}} = 2.6$ Hz, 2H, **ArH**), 7.55 (d, $^4J_{\text{HH}} = 2.6$ Hz, 2H, **ArH**), 7.37–7.36 (m, 2H, **ArH**), 7.22–7.20 (m, 2H, **ArH**), 7.10–7.06 (m, 3H, **ArH**), 7.02–6.97 (m, 4H, **ArH**), 5.08 (m, 2H, **CH₂**), 1.31 (s, 18H, **C(CH₃)₃**), 1.01 (s, 18H, **C(CH₃)₃**).

^{13}C NMR (125.77 MHz, toluene- d_8 , 343 K): δ 166.0 (**C=N**), 161.8 (**ArC**), 149.3 (**ArC**), 141.0 (**ArC**), 139.6 (**ArC**), 138.1 (**ArC**), 130.5 (**ArCH**), 128.2 (**ArCH**), 127.3 (**ArCH**), 126.3 (**ArC**), 125.6 (**ArCH**), 125.4 (**ArCH**), 121.7 (**ArCH**), 121.0 (**ArCH**), 110.7 (**ArC**), 110.3 (**ArCH**), 66.2 (**CH₂**), 35.1 (**C(CH₃)₃**), 34.6 (**C(CH₃)₃**), 31.7 (**C(CH₃)₃**), 29.4 (**C(CH₃)₃**).

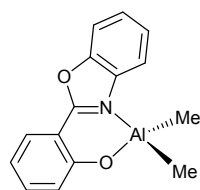


Fig. S2 ^1H NMR spectrum of **1a** in CDCl_3 at 298 K (* = solvent residue signal).

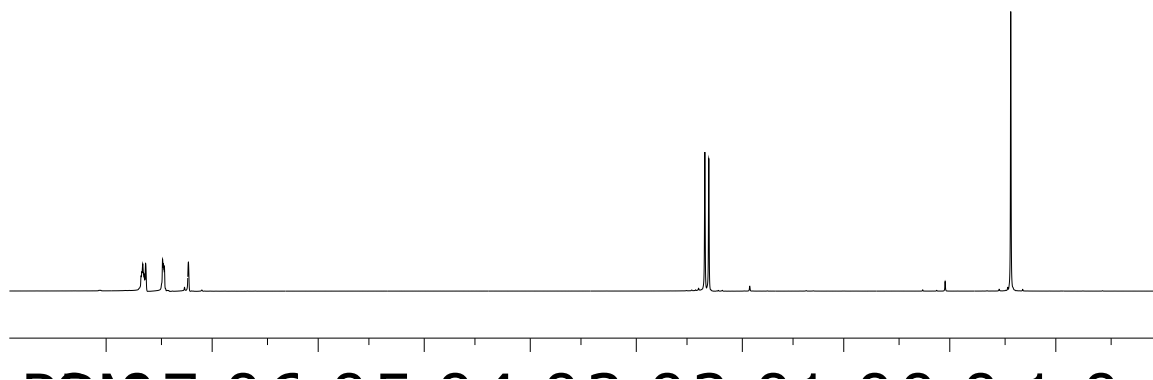
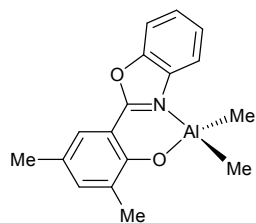


Fig. S3 ^1H NMR spectrum of **2a** in CDCl_3 at 298 K.

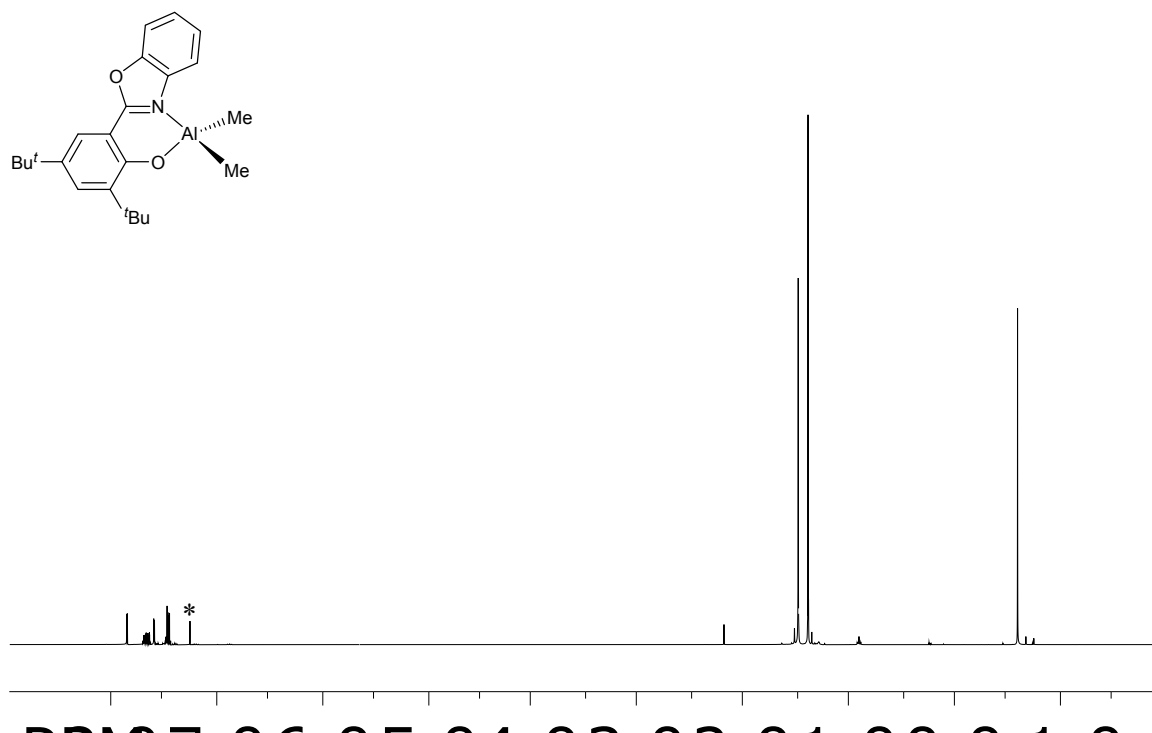


Fig. S4 ¹H NMR spectrum of **3a** in CDCl₃ at 298 K (* = solvent residue signal)

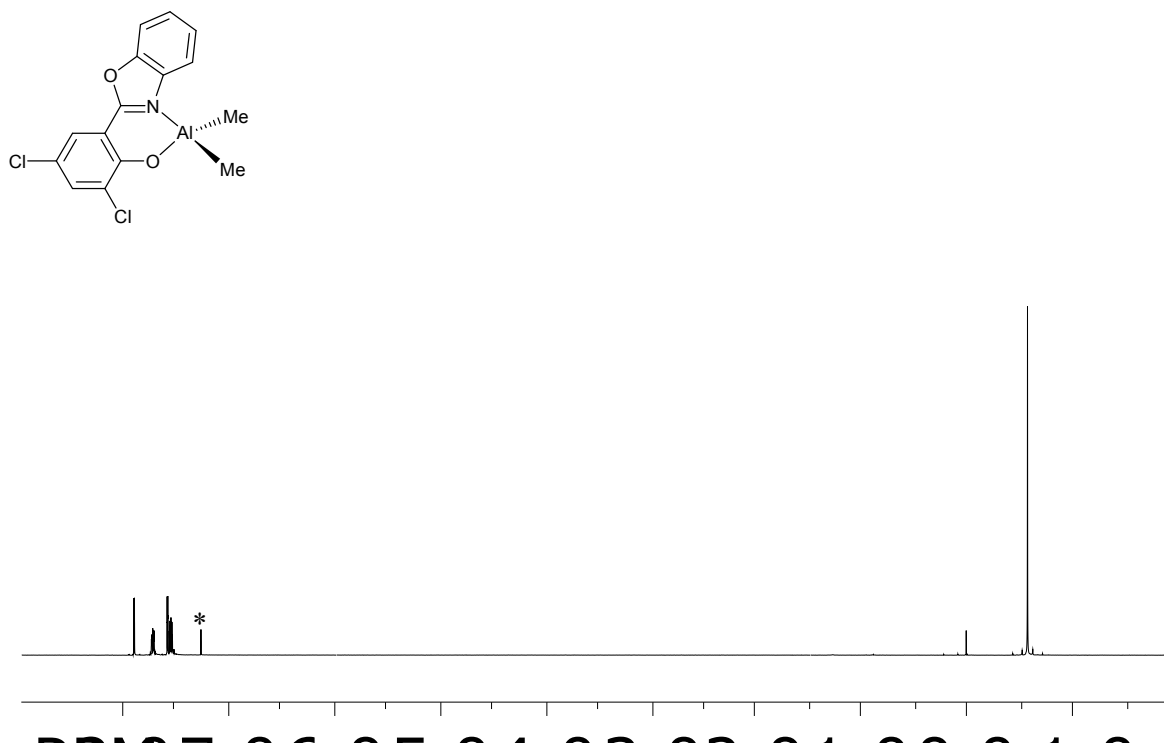


Fig. S5 ¹H NMR spectrum of **4a** in CDCl₃ at 298 K (* = solvent residue signal).

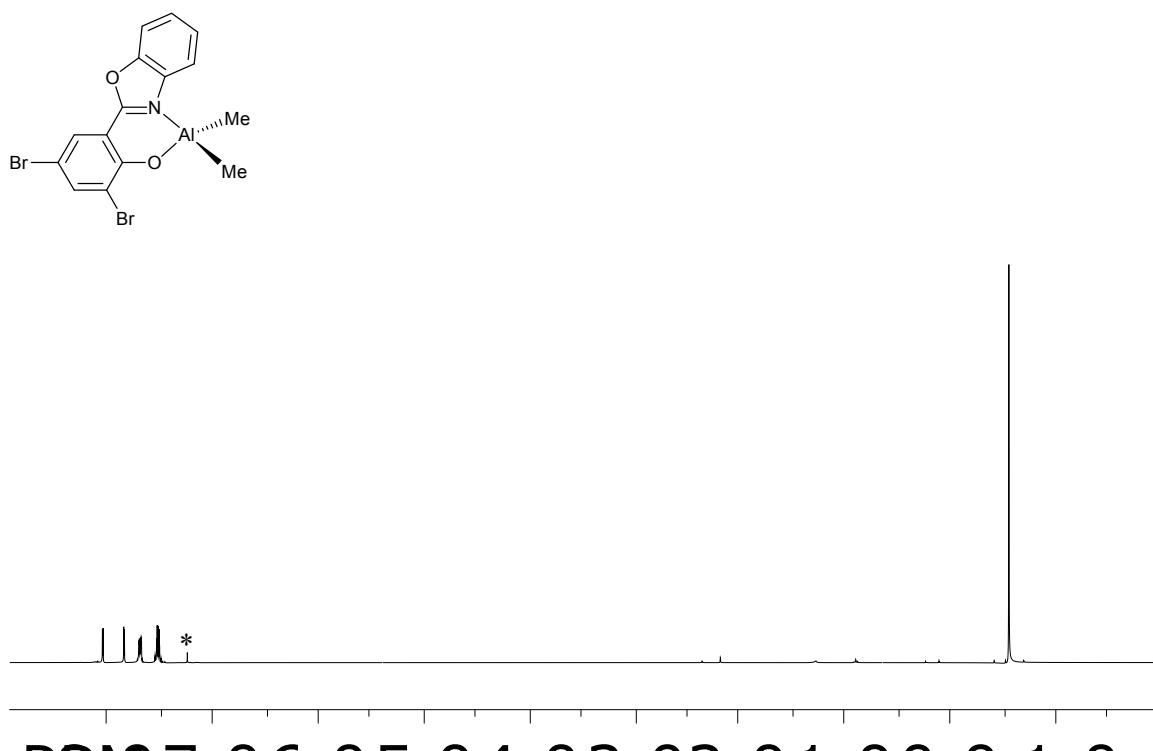


Fig. S6 ¹H NMR spectrum of **5a** in CDCl₃ at 298 K (* = solvent residue signal).

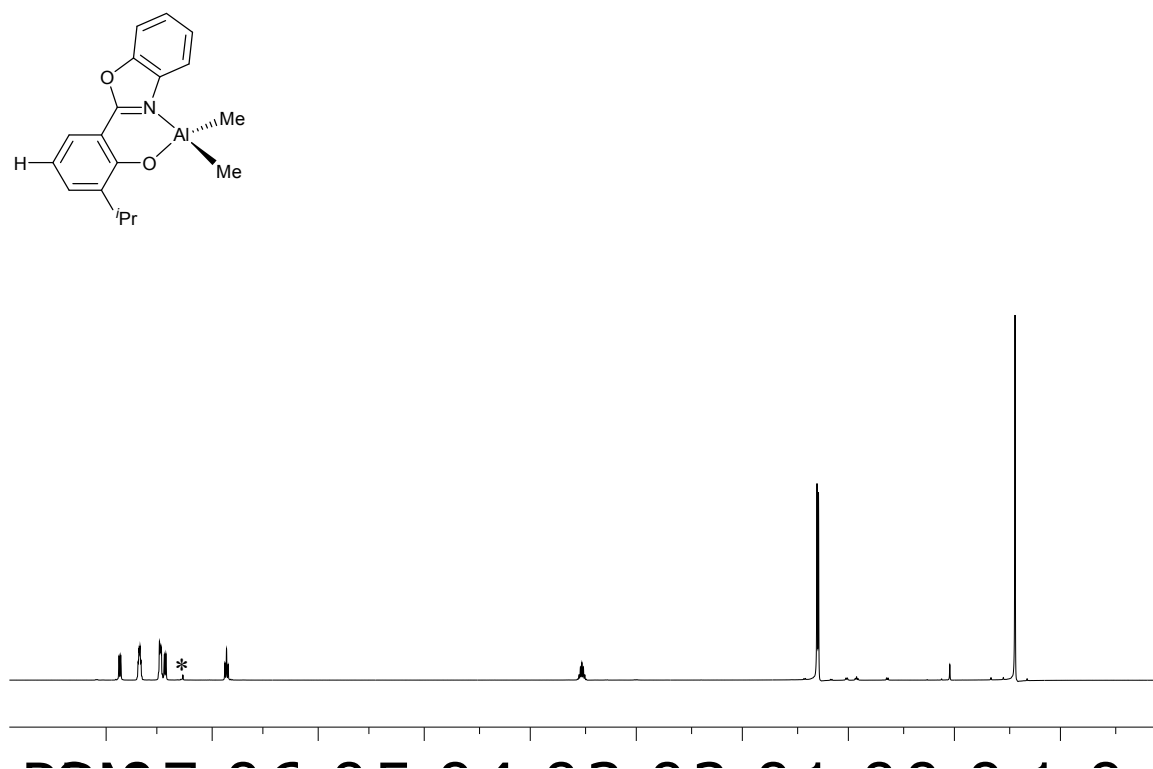


Fig. S7 ¹H NMR spectrum of **6a** in CDCl₃ at 298 K (* = solvent residue signal).

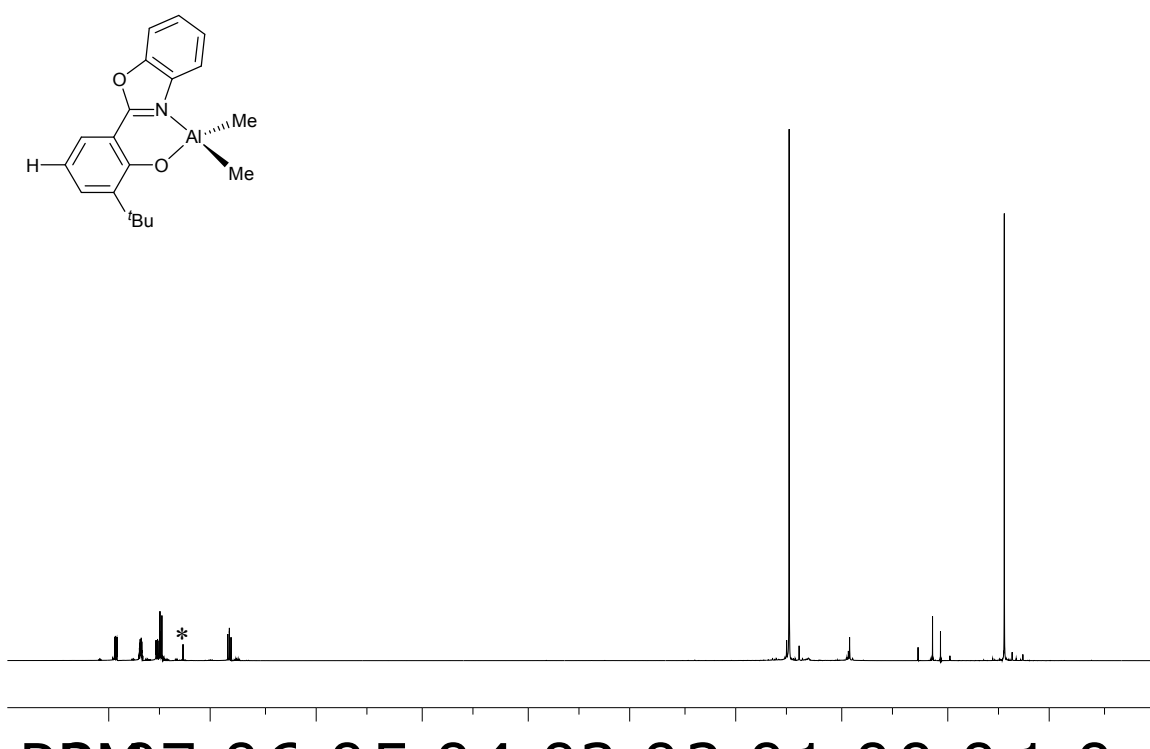


Fig. S8 ¹H NMR spectrum of **7a** in CDCl₃ at 298 K (* = solvent residue signal).

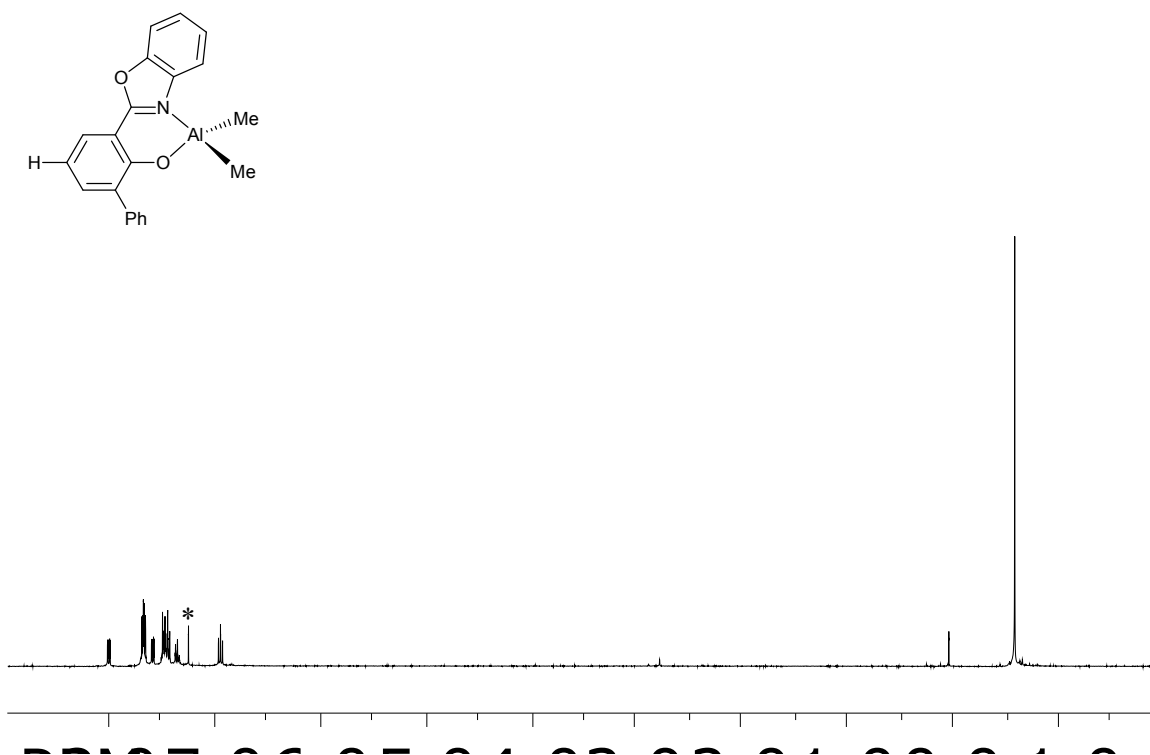


Fig. S9. ¹H NMR spectrum of **8a** in CDCl₃ at 298 K (* = solvent residue signal).

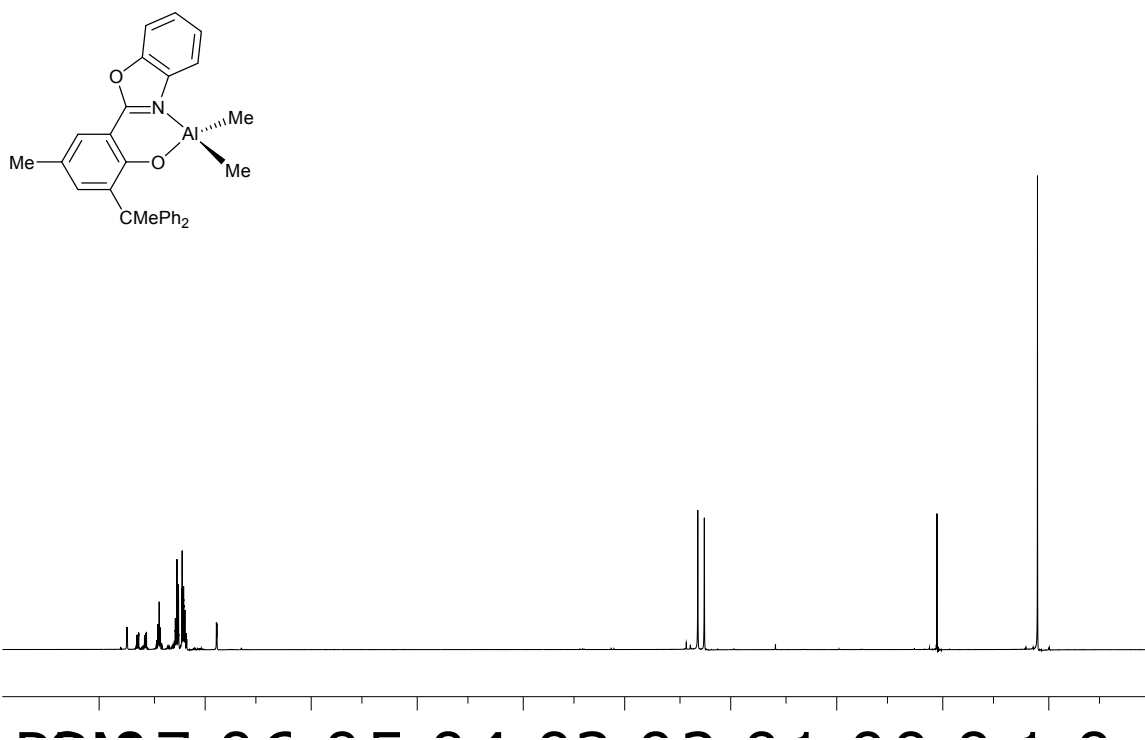


Fig. S10 ^1H NMR spectrum of **9a** in CDCl_3 at 298 K.

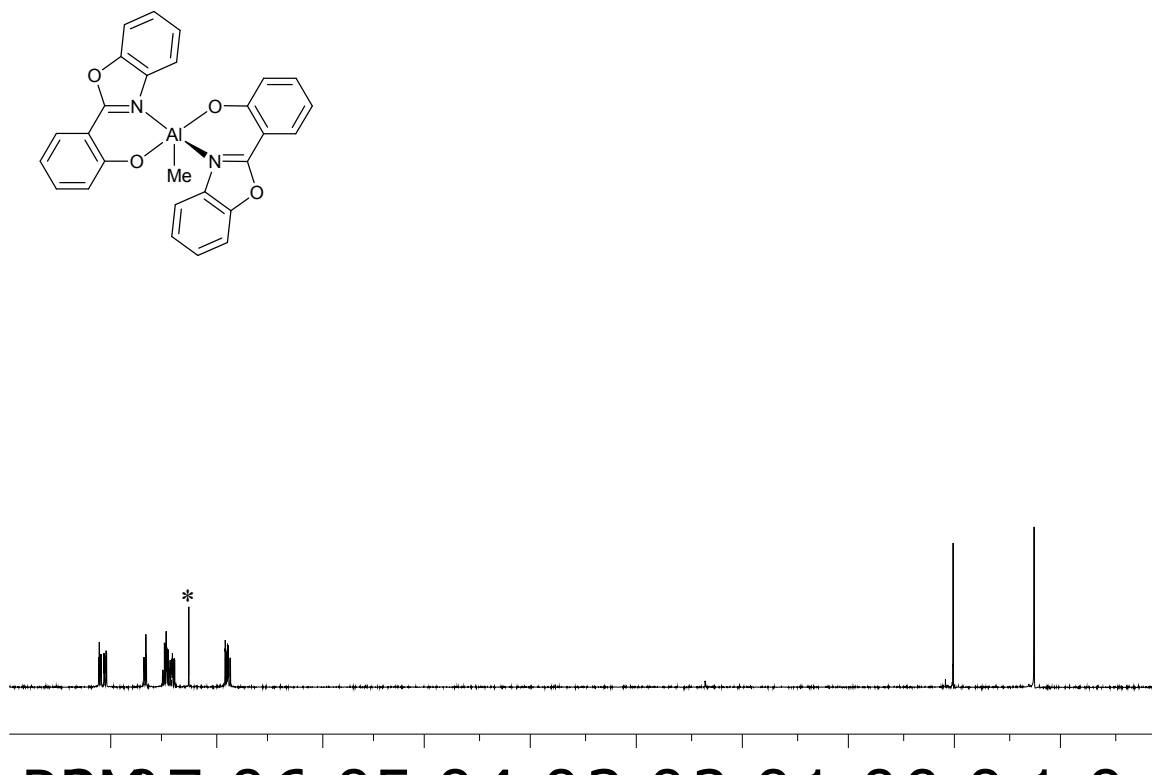


Fig. S11 ^1H NMR spectrum of **1b** in CDCl_3 at 298 K (* = solvent residue signal).

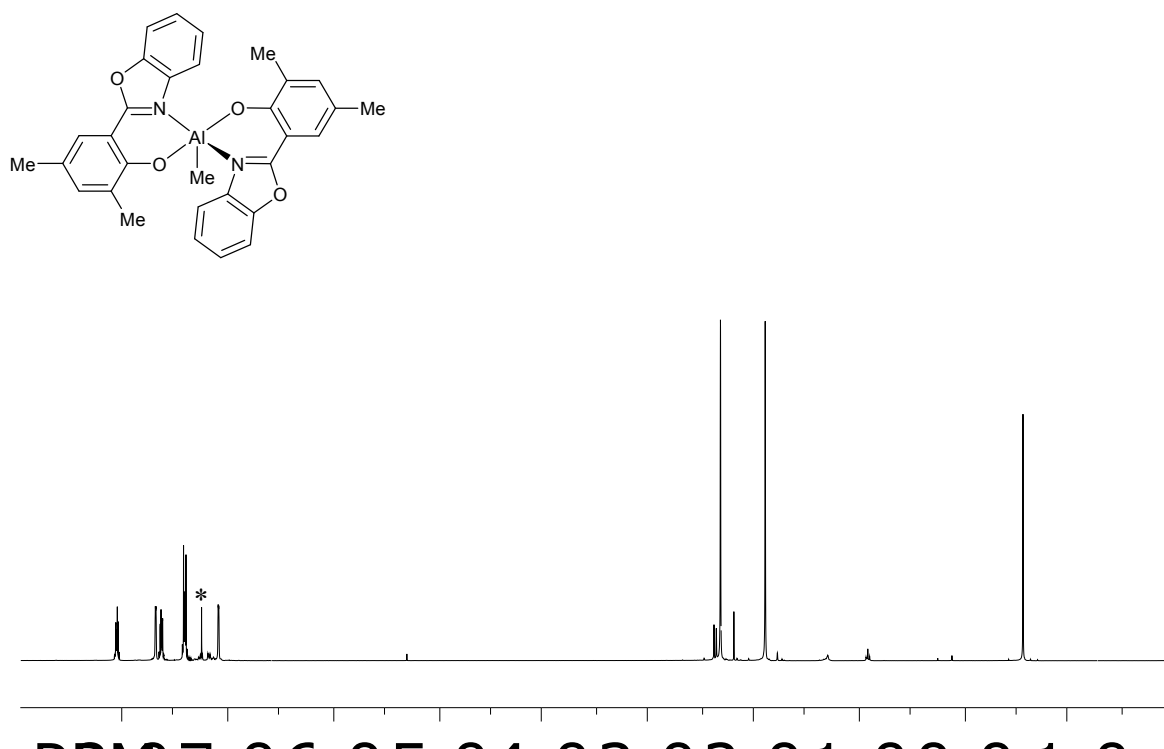


Fig. S12 ^1H NMR spectrum of **2b** in CDCl_3 at 298 K (* = solvent residue signal).

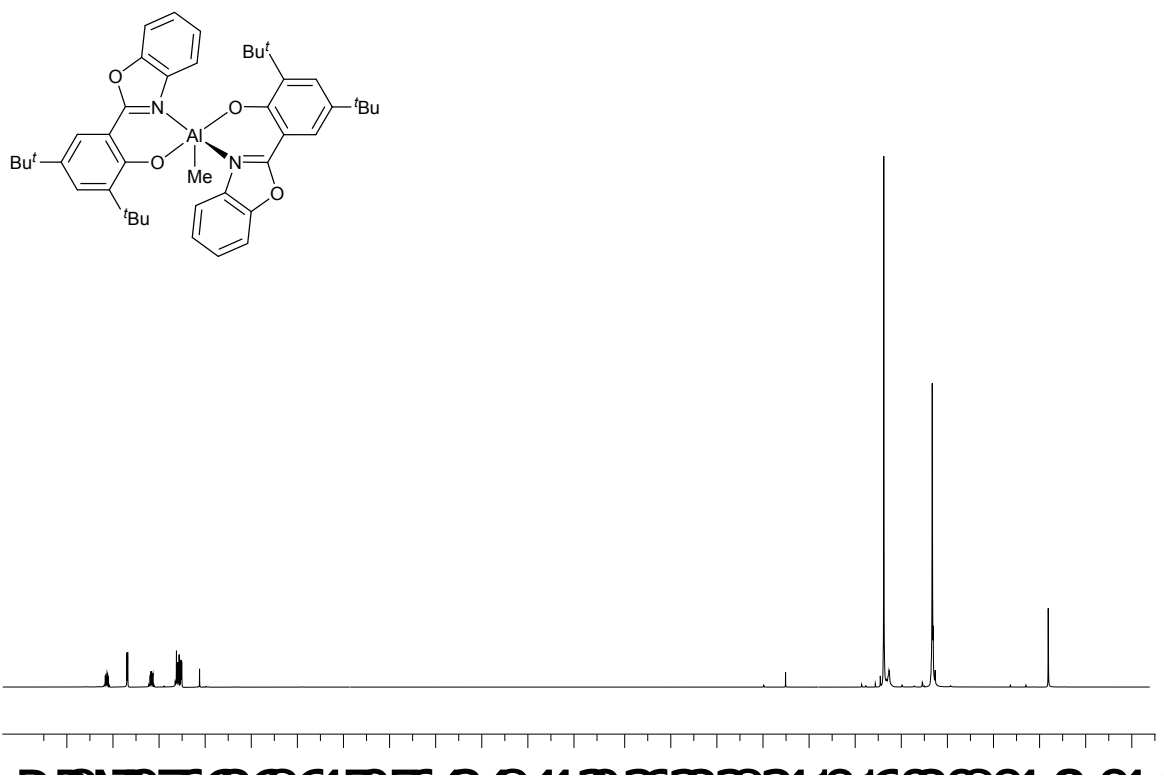


Fig. S13 ^1H NMR spectrum of **3b** in CDCl_3 at 298 K.

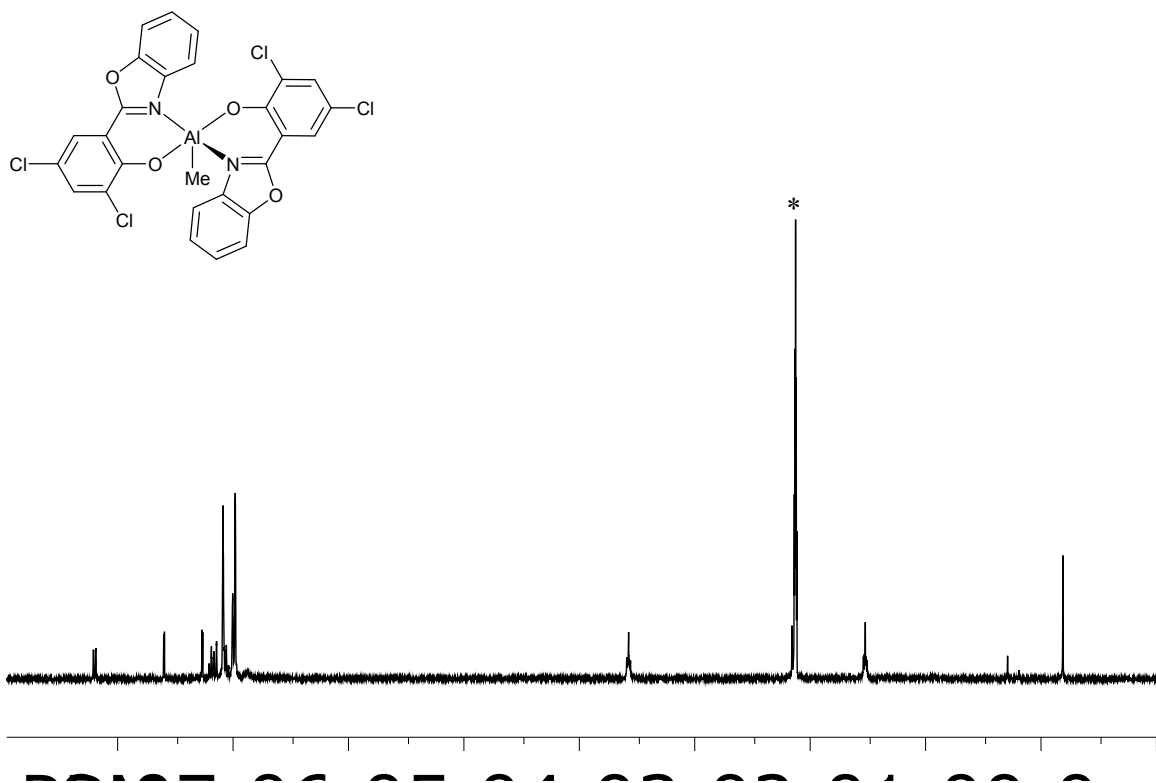


Fig. S14 ^1H NMR spectrum of **4b** in $\text{toluene-}d_8$ at 343 K (* = solvent residue signal).

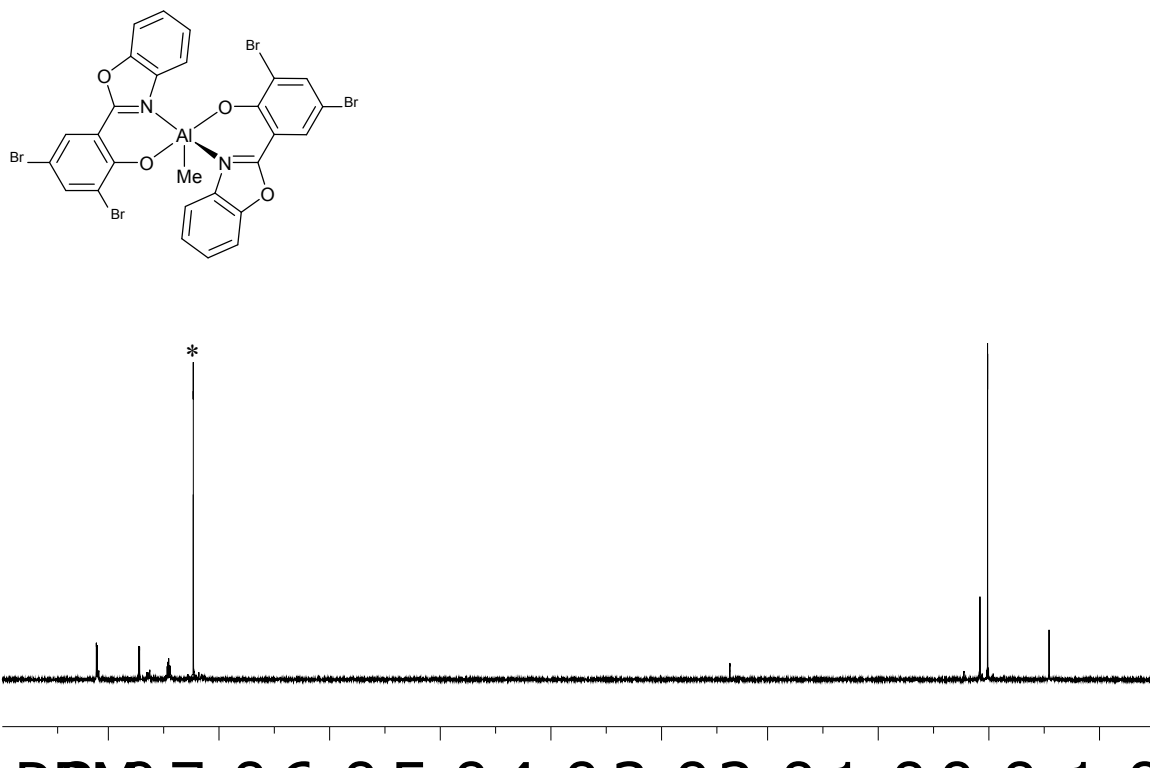


Fig. S15 ^1H NMR spectrum of **5b** in CDCl_3 at 298 K (* = solvent residue signal).

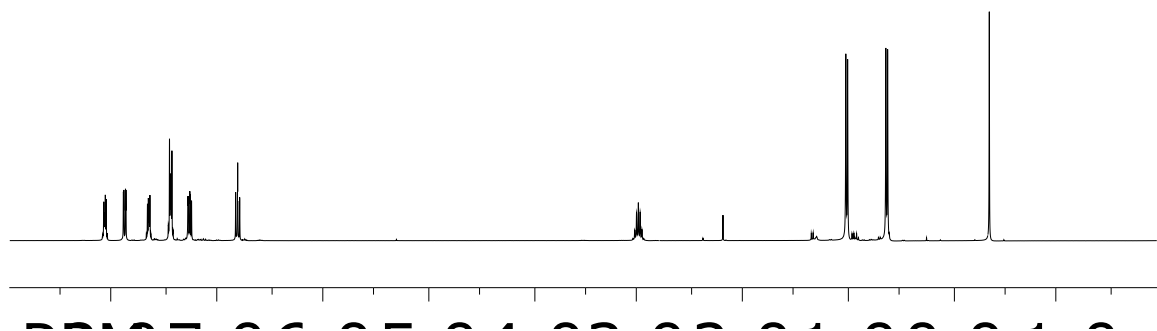
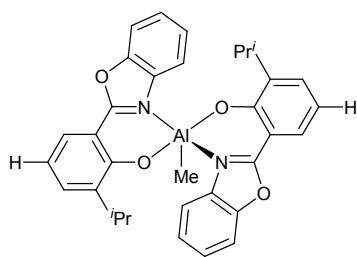


Fig. S16 ¹H NMR spectrum of **6b** in CDCl₃ at 298 K.

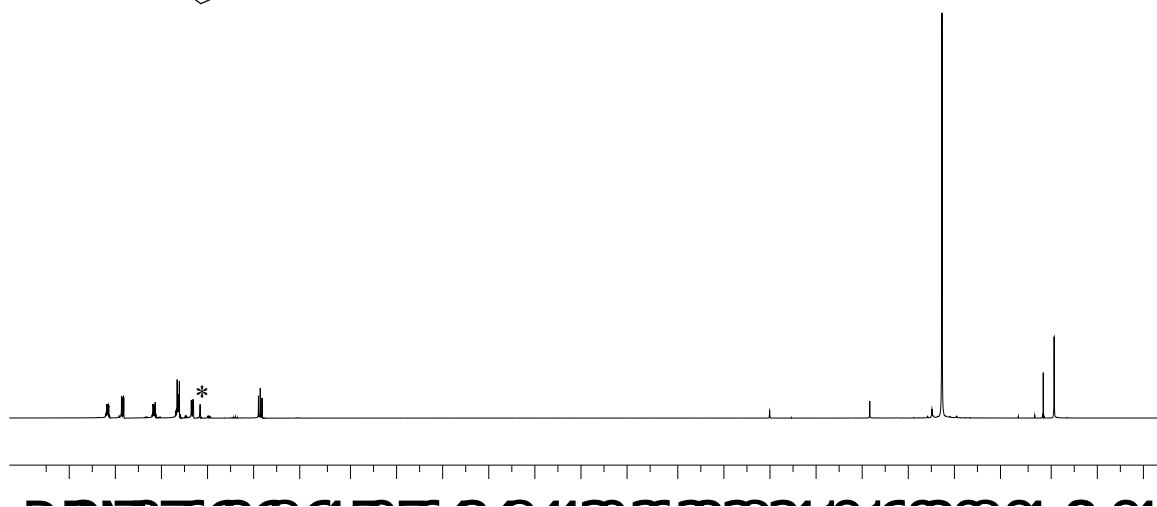
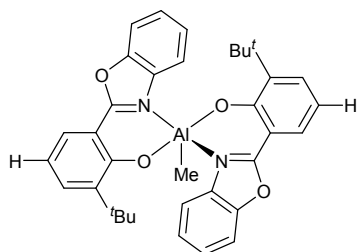


Fig. S17 ¹H NMR spectrum of **7b** in CDCl₃ at 298 K (* = solvent residue signal).

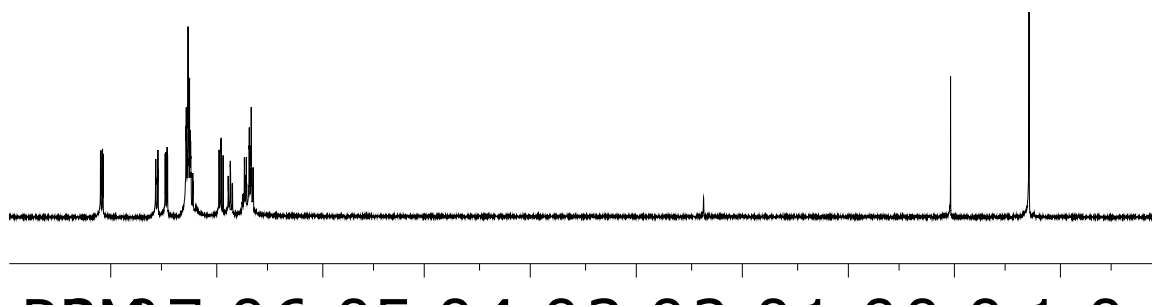
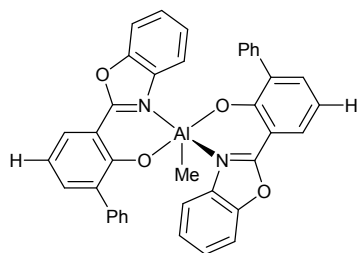


Fig. S18 ^1H NMR spectrum of **8b** in CDCl_3 at 298 K.

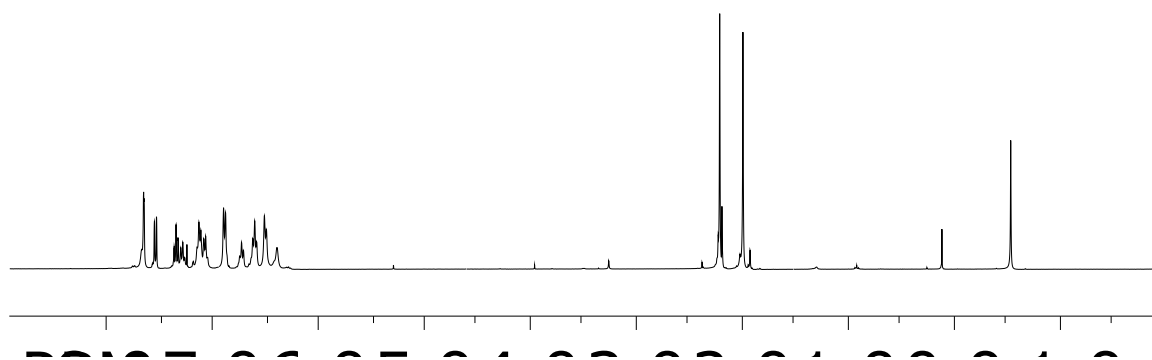
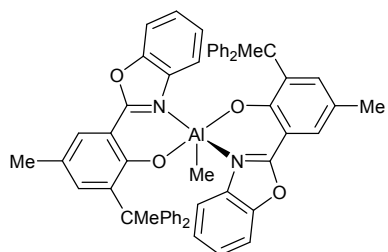


Fig. S19 ^1H NMR spectrum of **9b** in CDCl_3 at 298 K.

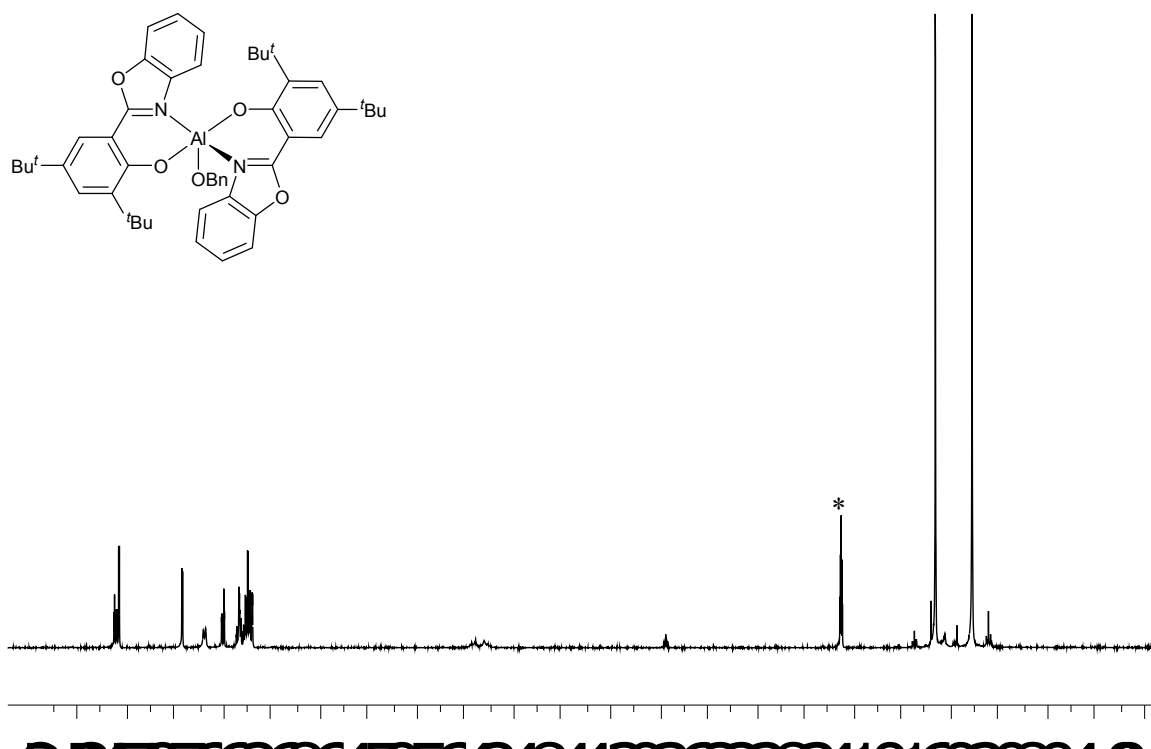


Fig. S20 ¹H NMR spectrum of **10** in toluene-*d*₈ at 343 K (* = solvent residue signal).

Table S1 Crystallographic data and structure refinement details for complex **7a**.

Empirical formula	C ₁₉ H ₂₂ AlNO ₂
Formula weight	323.25
Temperature (K)	100
Crystal size (mm)	0.180 × 0.220 × 0.260
Crystal system	monoclinic
Space group	P2/c
<i>a</i> (Å)	26.3261(13)
<i>b</i> (Å)	10.5969(4)
<i>c</i> (Å)	26.0751(11)
α (deg)	90
β (deg)	105.305(2)
γ (deg)	90
<i>V</i> (Å ³)	7016.3(5)
<i>Z</i>	16
Absorption coefficient (mm ⁻¹)	0.124
Calculated density (mg/m ³)	1.224
<i>F</i> (000)	2752
Theta range for data collection (deg)	0.80 to 25.06
Reflections collected	34479
Independent reflections	12422 [<i>R</i> (int) = 0.0474]
Number of observations [<i>I</i> > 2σ(<i>I</i>)]	7782
Goodness of fit on <i>F</i> ²	1.031
Final <i>R</i> indices [<i>I</i> > 2σ(<i>I</i>)]	<i>R</i> 1 = 0.0512 <i>wR</i> 2 = 0.1201
<i>R</i> indices (all data)	<i>R</i> 1 = 0.0970 <i>wR</i> 2 = 0.1431
Largest difference in peak and hole (e/Å ³)	0.28 and -0.35

Table S2 Bond lengths (Å) and bond angles (°) for complex **7a**.

Bond lengths (Å)					
Al1-O1	1.7697(18)	C1-C2	1.386(3)	C10-C11	1.386(4)
Al1-N1	1.951(2)	C6-C1	1.380(3)	C12-C11	1.387(3)
Al1-C19	1.951(3)	C2-C3	1.382(4)	C12-C13	1.419(3)
Al1-C18	1.956(3)	C4-C3	1.395(4)	C11-H11	0.93
C13-O1	1.334(3)	C5-C4	1.389(4)	C10-H10	0.93
C7-N1	1.317(3)	C6-C5	1.376(3)	C9-H9	0.93
C8-C7	1.441(3)	C5-H5	0.93	C14-C12	1.527(3)
C13-C8	1.415(3)	C4-H4	0.93	C14-C15	1.538(3)
O2-C7	1.356(3)	C3-H3	0.93	C14-C16	1.550(3)
N1-C1	1.410(3)	C2-H2	0.93	C17-C14	1.531(3)
C8-C9	1.401(3)	C10-C9	1.374(3)	C17-H17A	0.96
C15-H15A	0.96	C16-H16A	0.96	C17-H17B	0.96
C15-H15B	0.96	C16-H16B	0.96	C17-H17C	0.96
C15-H15C	0.96	C16-H16C	0.96	C19-H19B	0.96
C18-H18A	0.96	C18-H18C	0.96	C19-H19C	0.96
C18-H18B	0.96	C19-H19A	0.96		
Bond angles (°)					
O1-Al1-N1	92.08(9)	O1-Al1-C19	111.99(11)	N1-Al1-C19	107.97(11)
O1-Al1-C18	114.56(11)	N1-Al1-C18	108.75(10)	C19-Al1-C18	118.06(12)
C7-O2-C6	105.45(18)	C9-C10-C11	119.5(2)	C9-C10-H10	120.2
C11-C10-H10	120.2	C14-C17-H17A	109.5	C14-C17-H17B	109.5
H17A-C17-H17B	109.5	C14-C17-H17C	109.5	H17A-C17-H17C	109.5
H17B-C17-H17C	109.5	C12-C14-C17	110.3(2)	C12-C14-C15	112.0(2)
C17-C14-C15	107.2(2)	C12-C14-C16	109.5(2)	C17-C14-C16	110.8(2)
C15-C14-C16	107.0(2)	C11-C12-C13	116.9(2)	C11-C12-C14	122.2(2)
C13-C12-C14	120.9(2)	O1-C13-C8	120.5(2)	C9-C8-C13	120.9(2)
O1-C13-C12	120.0(2)	C8-C13-C12	119.5(2)	C9-C8-C7	119.0(2)
C13-C8-C7	120.0(2)	N1-C7-O2	113.3(2)	N1-C7-C8	128.2(2)
O2-C7-C8	118.4(2)	C5-C6-C1	124.0(2)	C5-C6-O2	128.0(2)
C1-C6-O2	108.0(2)	C6-C5-C4	115.0(2)	C6-C5-H5	122.5
C4-C5-H5	122.5	C5-C4-C3	121.8(3)	C5-C4-H4	119.1
C3-C4-H4	119.1	C14-C15-H15B	109.5	C1-N1-Al1	131.08(16)
C14-C16-H16A	109.5	H15A-C15-H15B	109.5	C6-C1-C2	120.8(3)
C14-C16-H16B	109.5	C14-C15-H15C	109.5	C6-C1-N1	107.5(2)
H16A-C16-H16B	109.5	H15A-C15-H15C	109.5	C2-C1-N1	131.7(2)
C14-C16-H16C	109.5	H15B-C15-H15C	109.5	C3-C2-C1	116.5(2)
H16A-C16-H16C	109.5	C13-O1-Al1	135.49(16)	C3-C2-H2	121.8
H16B-C16-H16C	109.5	C7-N1-C1	105.8(2)	C1-C2-H2	121.8
C14-C15-H15A	109.5	C7-N1-Al1	122.99(17)	C2-C3-C4	121.9(3)
C2-C3-H3	119.0	C4-C3-H3	119.0	C10-C9-C8	119.4(2)
C10-C9-H9	120.3	C10-C11-H11	118.1	C12-C11-H11	118.1
Al1-C18-H18A	109.5	Al1-C18-H18C	109.5	H19A-C19-H19B	109.5
Al1-C18-H18B	109.5	H18A-C18-H18C	109.5	Al1-C19-H19C	109.5
H18A-C18-H18B	109.5	H18B-C18-H18C	109.5	H19A-C19-H19C	109.5
Al1-C19-H19A	109.5	Al1-C19-H19B	109.5	H19B-C19-H19C	109.5

Table S3 Crystallographic data and structure refinement details for complex **1b**.

Empirical formula	C ₂₇ H ₁₉ AlN ₂ O ₄ ·C ₇ H ₈
Formula weight	554.55
Temperature (K)	100
Crystal size (mm)	0.240 x 0.320 x 0.460
Crystal system	monoclinic
Space group	P2 ₁ /c
<i>a</i> (Å)	12.1416(15)
<i>b</i> (Å)	21.238(2)
<i>c</i> (Å)	10.7010(11)
α (deg)	90
β (deg)	93.260(4)
γ (deg)	90
<i>V</i> (Å ³)	2754.9(5)
<i>Z</i>	4
Absorption coefficient (mm ⁻¹)	0.117
Calculated density (mg/m ³)	1.337
<i>F</i> (000)	1160
Theta range for data collection (deg)	5.1 to 55
Reflections collected	16300
Independent reflections	6260 [<i>R</i> (int) = 0.0459]
Number of observations [$>2\sigma(I)$]	4874
Goodness of fit on <i>F</i> ²	1.044
Final <i>R</i> indices [$I > 2\sigma(I)$]	<i>R</i> 1 = 0.0422 <i>wR</i> 2 = 0.1058
<i>R</i> indices (all data)	<i>R</i> 1 = 0.0574 <i>wR</i> 2 = 0.1154
Largest difference in peak and hole (e/Å ³)	0.35 and -0.28

Table S4 Bond lengths (Å) and bond angles (°) for complex **1b**.

Bond lengths (Å)					
A11-O3	1.7891(12)	A11-N2	2.0472(12)	O2-C7	1.3621(17)
A11-O1	1.7873(12)	A11-N1	2.0666(13)	O1-C1	1.3240(18)
A11-C27	1.9574(16)	O2-C8	1.3804(18)	O3-C14	1.3272(17)
O3-C14	1.3272(17)	O4-C21	1.3818(18)	N2-C7	1.3074(18)
N2-C13	1.4057(19)	N1-C20	1.3097(18)	C24-H24	0.9300
N1-C26	1.4049(19)	C7-C6	1.434(2)	C23-C22	1.386(2)
C4-C5	1.370(2)	C4-C3	1.389(2)	C16-C17	1.392(2)
C4-H4	0.9300	C5-C6	1.404(2)	C10-C9	1.385(2)
C19-C14	1.416(2)	C6-C1	1.410(2)	C10-C11	1.395(2)
C15-C16	1.378(2)	C15-C14	1.398(2)	C10-H10	0.9300
C15-H15	0.9300	C26-C25	1.382(2)	C11-C12	1.388(2)
C26-C21	1.381(2)	C25-C24	1.384(2)	C1-C2	1.403(2)
C25-H25	0.9300	C24-C23	1.392(2)	C12-C13	1.386(2)
C12-H12	0.9300	C13-C8	1.385(2)	C27-H27A	0.9600
C8-C9	1.376(2)	C16-H16	0.9300	C3-C2	1.375(2)
C3-H3	0.9300	C17-C18	1.372(2)	C20-C19	1.436(2)
C21-C22	1.381(2)	C22-H22	0.9300	C19-C18	1.404(2)
Bond angles (°)					
O3-A11-O1	121.02(6)	O3-A11-C27	119.15(7)	C8-C9-H9	122.4
O1-A11-C27	119.79(8)	O3-A11-N2	85.89(5)	C24-C23-C22	121.70(16)
O1-A11-N2	88.08(5)	C27-A11-N2	98.15(6)	C9-C10-C11	121.50(15)
O3-A11-N1	87.46(5)	O1-A11-N1	85.15(5)	C9-C10-H10	119.3
C27-A11-N1	95.50(6)	N2-A11-N1	166.35(5)	C2-C3-C4	120.63(16)
C7-O2-C8	104.87(11)	C1-O1-A11	137.09(10)	C12-C11-C10	122.24(16)
C14-O3-A11	136.6(10)	C20-O4-C21	104.90(11)	C12-C11-H11	118.9
C7-N2-C13	105.48(12)	C7-N2-A11	125.02(10)	C2-C1-C6	117.91(14)
C13-N2-A11	129.43(10)	C20-N1-C26	105.82(12)	C13-C12-C11	116.48(15)
C20-N1-A11	124.98(10)	C26-N1-A11	129.14(10)	C13-C12-H12	121.8
N2-C7-O2	113.96(13)	N2-C7-C6	127.58(13)	C2-C3-H3	119.7
O2-C7-C6	118.45(12)	C5-C4-C3	119.68(15)	C12-C13-C8	120.15(14)
C5-C4-H4	120.2	C3-C2-C1	121.12(15)	C12-C13-N2	132.22(14)
C4-C5-C6	120.68(16)	C4-C5-H5	119.7	C8-C13-N2	107.59(13)
N1-C20-O4	113.51(13)	C5-C6-C1	119.98(14)	A11-C27-H27A	109.5
C5-C6-C7	120.91(14)	C1-C6-C7	119.09(13)	C9-C8-O2	127.49(14)
C16-C15-C14	120.92(14)	C16-C15-H15	119.5	C9-C8-C13	124.39(14)
N1-C20-C19	127.40(13)	C25-C26-C21	120.32(15)	A11-C27-H27C	109.5
C25-C26-N1	132.19(14)	C21-C26-N1	107.48(13)	O2-C8-C13	108.09(12)
C26-C25-C24	117.02(15)	O4-C20-C19	119.09(12)	C8-C9-C10	115.25(15)
C24-C25-H25	121.5	C25-C24-C23	121.74(16)	O1-C1-C2	119.11(14)
O4-C21-C26	108.30(13)	C22-C21-C26	123.87(15)	C18-C17-H17	120.1
C21-C22-C23	115.33(15)	C21-C22-H22	122.3	C17-C18-C19	120.44(14)
C23-C22-H22	122.3	C18-C19-C14	120.00(14)	C19-C18-H18	119.8
C18-C19-C20	121.07(13)	C14-C19-C20	118.92(13)	O3-C14-C19	123.04(14)
C15-C16-C17	120.69(15)	C15-C16-H16	119.7	C21-C22-C23	115.33(15)
C17-C16-H16	119.7	C18-C17-C16	119.80(15)	C18-C17-H17	120.1
C23-C24-H24	119.1	C16-C17-H17	120.1	O1-C1-C6	122.97(14)
O3-C14-C15	118.82(13)	C17-C18-H18	119.8	C15-C14-C19	118.13(13)

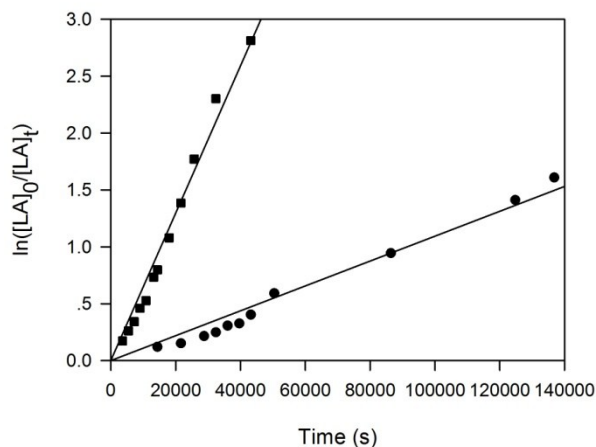


Fig. S21 Semilogarithmic plots of *rac*-lactide conversion *versus* time in toluene at 70 °C with complexes **2a** (■) and **2b** (●) ($[LA]_0/[Al]/[PhCH_2OH] = 50:1:1$, $[LA]_0 = 0.42$ M, $[Al] = 8.33$ mM).

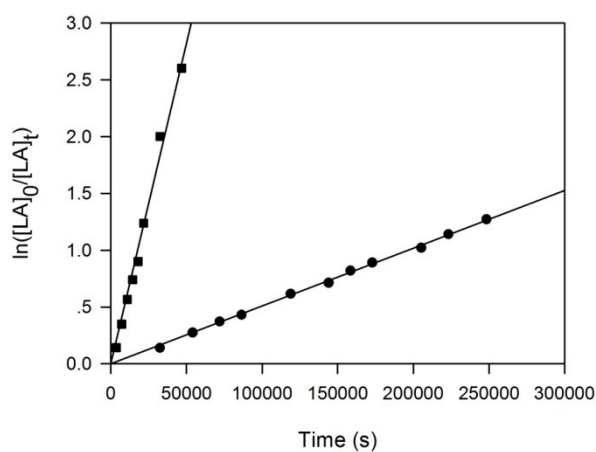


Fig. S22 Semilogarithmic plots of *rac*-lactide conversion *versus* time in toluene at 70 °C with complexes **3a** (■) and **3b** (●) ($[LA]_0/[Al]/[PhCH_2OH] = 50:1:1$, $[LA]_0 = 0.42$ M, $[Al] = 8.33$ mM).

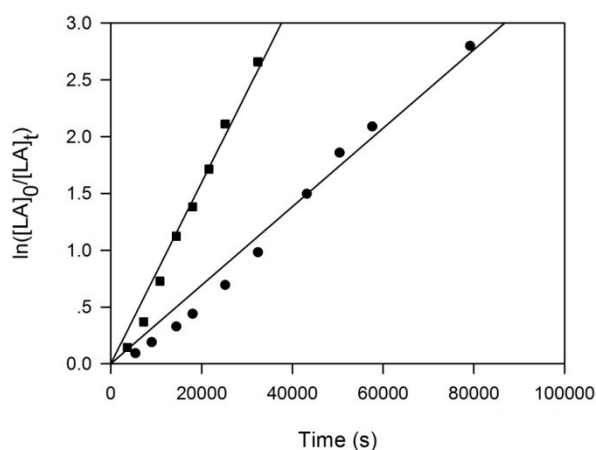


Fig. S23 Semilogarithmic plots of *rac*-lactide conversion *versus* time in toluene at 70 °C with complexes **4a** (■) and **4b** (●) ($[LA]_0/[Al]/[PhCH_2OH] = 50:1:1$, $[LA]_0 = 0.42$ M, $[Al] = 8.33$ mM).

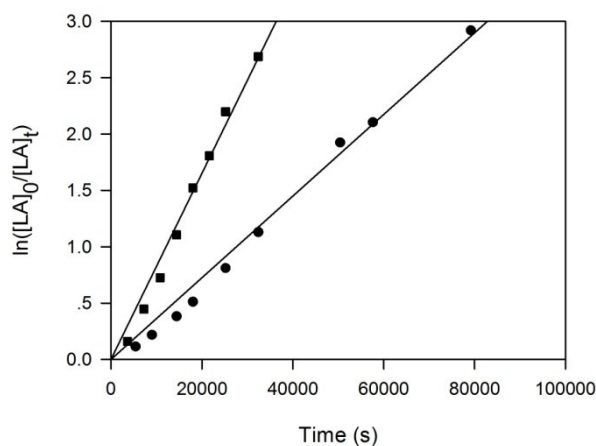


Fig. S24 Semilogarithmic plots of *rac*-lactide conversion *versus* time in toluene at 70 °C with complexes **5a** (■) and **5b** (●) ($[LA]_0/[Al]/[PhCH_2OH] = 50:1:1$, $[LA]_0 = 0.42$ M, $[Al] = 8.33$ mM).

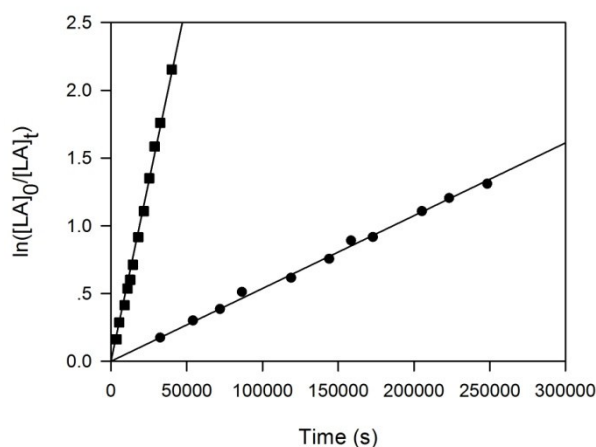


Fig. S25 Semilogarithmic plots of *rac*-lactide conversion *versus* time in toluene at 70 °C with complexes **6a** (■) and **6b** (●) ($[LA]_0/[Al]/[PhCH_2OH] = 50:1:1$, $[LA]_0 = 0.42$ M, $[Al] = 8.33$ mM).

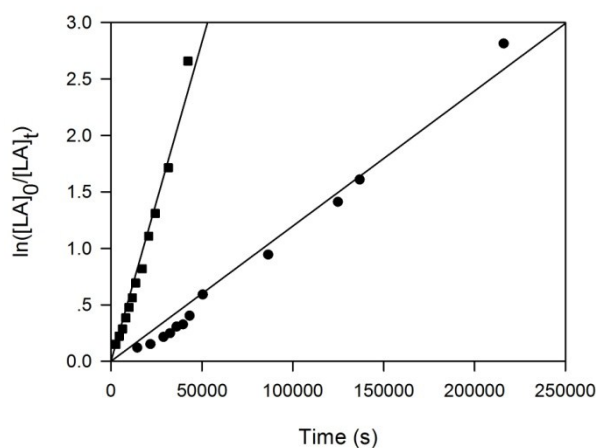


Fig. S26 Semilogarithmic plots of *rac*-lactide conversion *versus* time in toluene at 70 °C with complexes **7a** (■) and **7b** (●) ($[LA]_0/[Al]/[PhCH_2OH] = 50:1:1$, $[LA]_0 = 0.42$ M, $[Al] = 8.33$ mM).

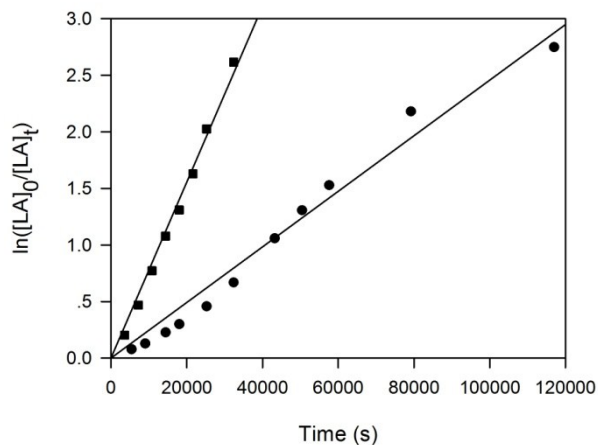


Fig. S27 Semilogarithmic plots of *rac*-lactide conversion *versus* time in toluene at 70 °C with complexes **8a** (■) and **8b** (●) ($[LA]_0/[Al]/[PhCH_2OH] = 50:1:1$, $[LA]_0 = 0.42$ M, $[Al] = 8.33$ mM).

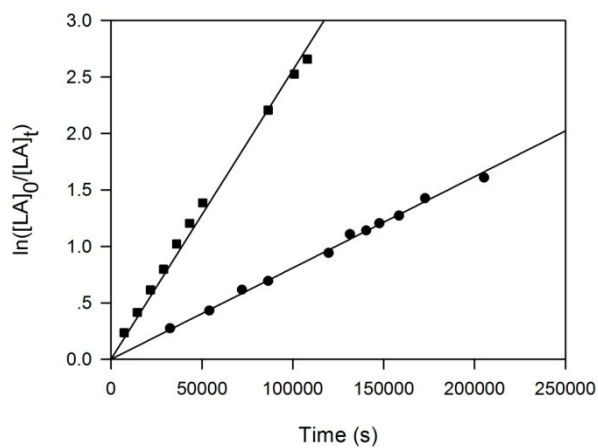


Fig. S28 Semilogarithmic plots of *rac*-lactide conversion *versus* time in toluene at 70 °C with complexes **9a** (■) and **9b** (●) ($[LA]_0/[Al]/[PhCH_2OH] = 50:1:1$, $[LA]_0 = 0.42$ M, $[Al] = 8.33$ mM).

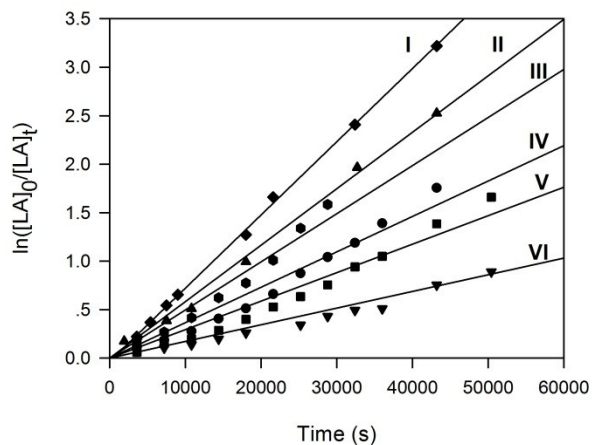


Fig. S29 Semilogarithmic plots of the *rac*-lactide conversion *versus* time in toluene at 70 °C with complex **1b**/PhCH₂OH as an initiator ($[LA]_0 = 0.42$ M: **I**, $[Al] = 33.32$ mM, $[LA]_0/[Al] = 13$; **II**, $[Al] = 24.99$ mM, $[LA]_0/[Al] = 17$; **III**, $[Al] = 20.82$ mM, $[LA]_0/[Al] = 20$; **IV**, $[Al] = 16.66$ mM, $[LA]_0/[Al] = 25$; **V**, $[Al] = 12.50$ mM, $[LA]_0/[Al] = 34$; **VI**, $[Al] = 8.33$ mM, $[LA]_0/[Al] = 50$).

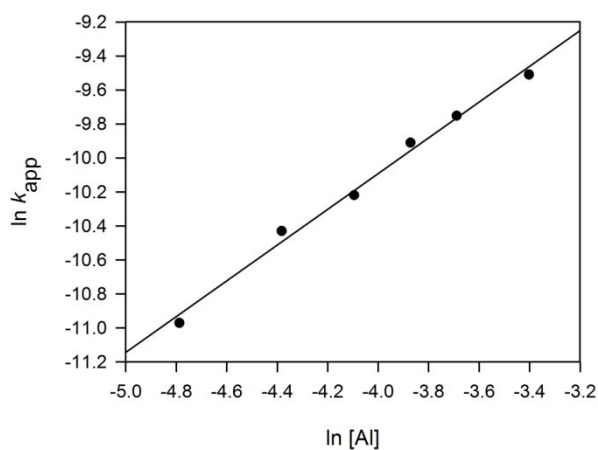


Fig. S30 Plot of $\ln k_{app}$ *versus* $\ln [Al]$ for the polymerization of *rac*-lactide with complex **1b**/PhCH₂OH as an initiator (toluene, 70 °C, $[LA]_0 = 0.42$ M).

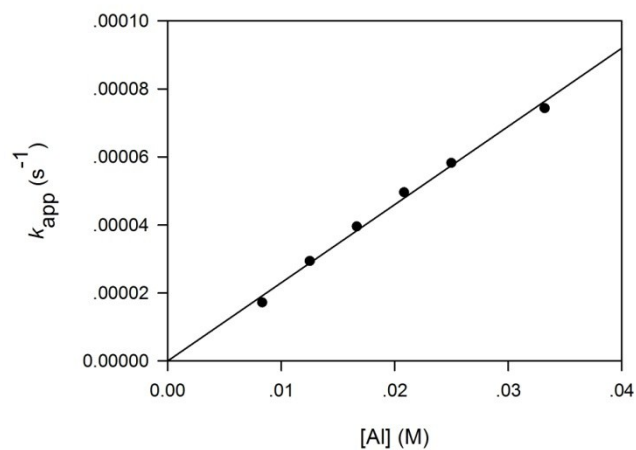


Fig. S31 Plot of k_{app} versus $[AI]$ for the polymerization of *rac*-lactide with complex **1b**/PhCH₂OH as an initiator (toluene, 70 °C, $[LA]_0 = 0.42$ M).

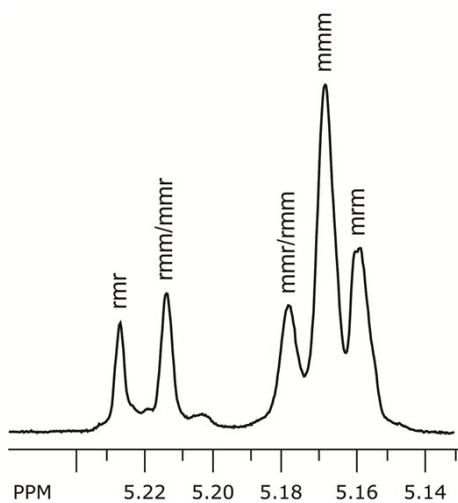


Fig. S32 Homonuclear decoupled ¹H NMR spectrum of the methine region of PLA prepared from *rac*-lactide at 70 °C in toluene (500 MHz, CDCl₃) with **1a**/PhCH₂OH.

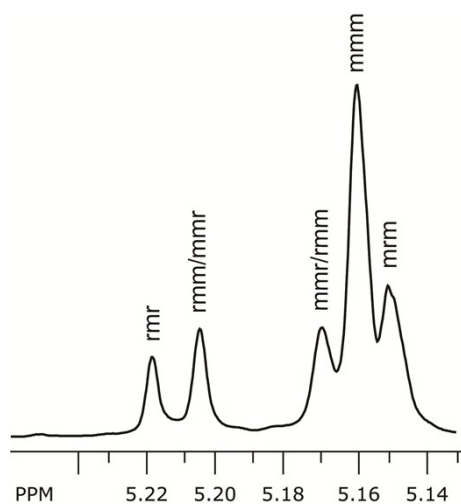


Fig. S33 Homonuclear decoupled ^1H NMR spectrum of the methine region of PLA prepared from *rac*-lactide at 70 °C in toluene (500 MHz, CDCl_3) with **1b**/PhCH₂OH.

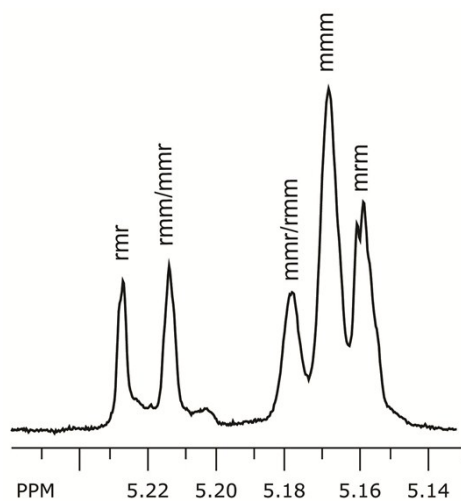


Fig. S34 Homonuclear decoupled ^1H NMR spectrum of the methine region of PLA prepared from *rac*-lactide at 70 °C in toluene (500 MHz, CDCl_3) with **2a**/PhCH₂OH.

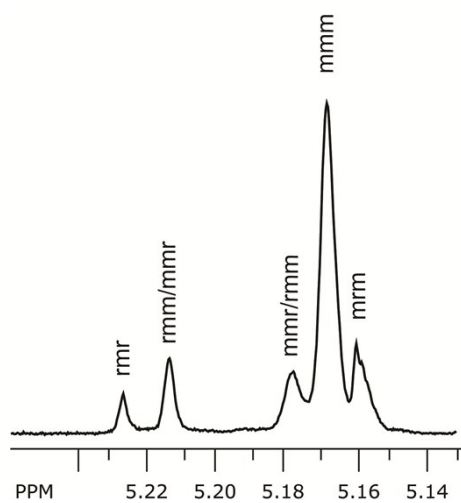


Fig. S35 Homonuclear decoupled ^1H NMR spectrum of the methine region of PLA prepared from *rac*-lactide at 70 °C in toluene (500 MHz, CDCl_3) with **2b**/PhCH₂OH.

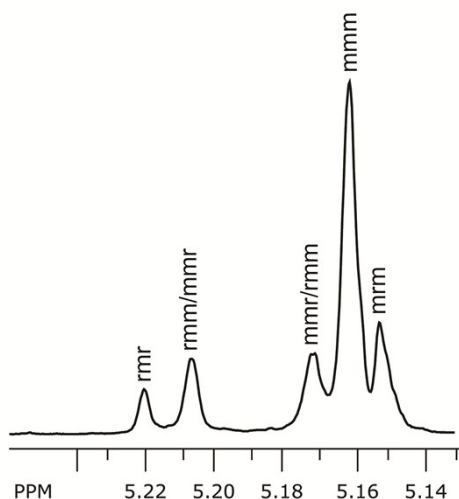


Fig. S36 Homonuclear decoupled ^1H NMR spectrum of the methine region of PLA prepared from *rac*-lactide at 70 °C in toluene (500 MHz, CDCl_3) with **3a**/ PhCH_2OH .

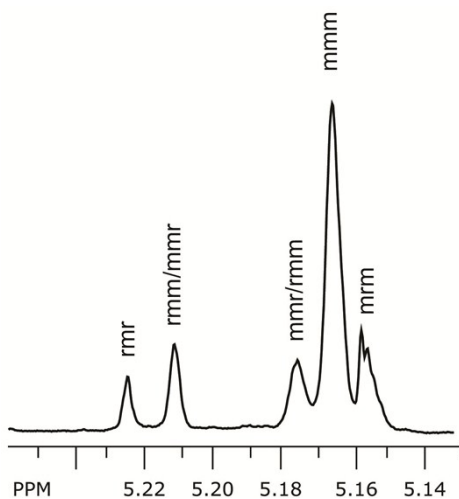


Fig. S37 Homonuclear decoupled ^1H NMR spectrum of the methine region of PLA prepared from *rac*-lactide at 70 °C in toluene (500 MHz, CDCl_3) with **3b**/ PhCH_2OH .

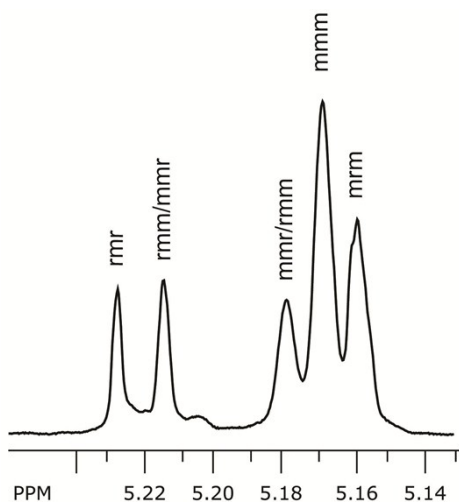


Fig. S38 Homonuclear decoupled ^1H NMR spectrum of the methine region of PLA prepared from *rac*-lactide at 70 °C in toluene (500 MHz, CDCl_3) with **4a**/ PhCH_2OH .

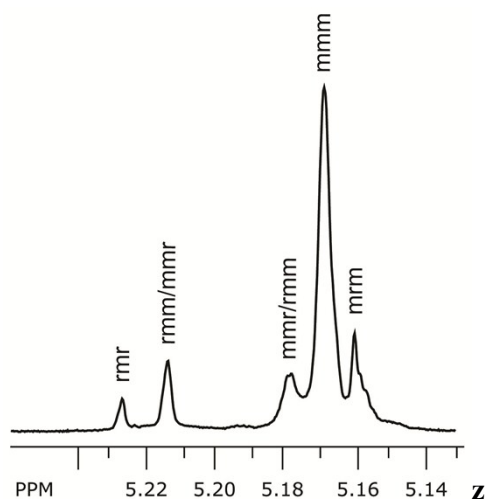


Fig. S39 Homonuclear decoupled ^1H NMR spectrum of the methine region of PLA prepared from *rac*-lactide at 70 °C in toluene (500 MHz, CDCl_3) with **4b**/ PhCH_2OH .

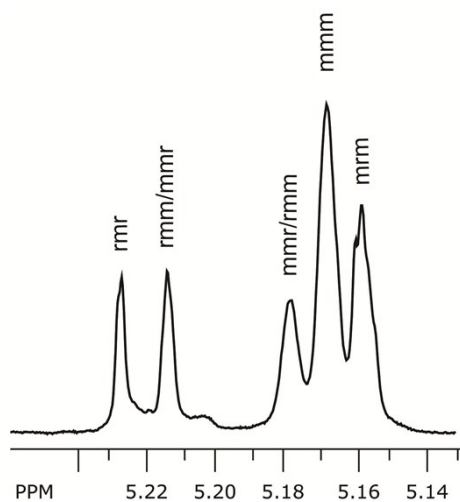


Fig. S40 Homonuclear decoupled ^1H NMR spectrum of the methine region of PLA prepared from *rac*-lactide at 70 °C in toluene (500 MHz, CDCl_3) with **5a**/ PhCH_2OH .

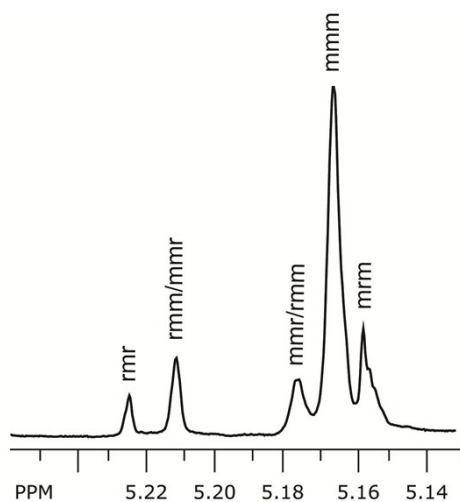


Fig. S41 Homonuclear decoupled ^1H NMR spectrum of the methine region of PLA prepared from *rac*-lactide at 70 °C in toluene (500 MHz, CDCl_3) with **5b**/ PhCH_2OH .

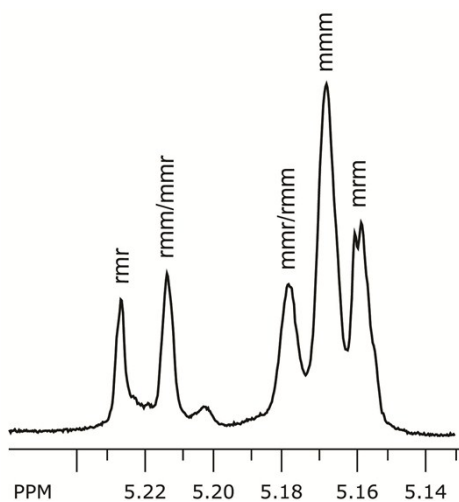


Fig. S42 Homonuclear decoupled ^1H NMR spectrum of the methine region of PLA prepared from *rac*-lactide at 70 °C in toluene (500 MHz, CDCl_3) with **6a**/ PhCH_2OH .

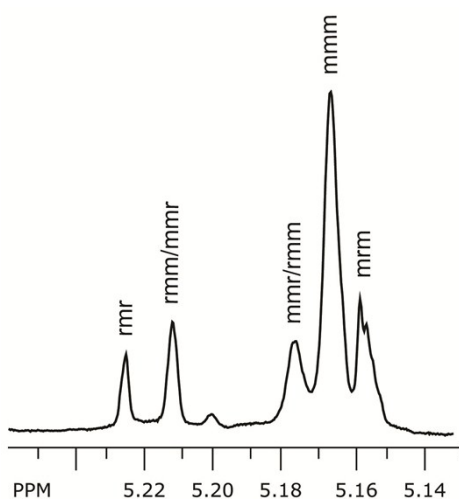


Fig. S43 Homonuclear decoupled ^1H NMR spectrum of the methine region of PLA prepared from *rac*-lactide at 70 °C in toluene (500 MHz, CDCl_3) with **6b**/ PhCH_2OH .

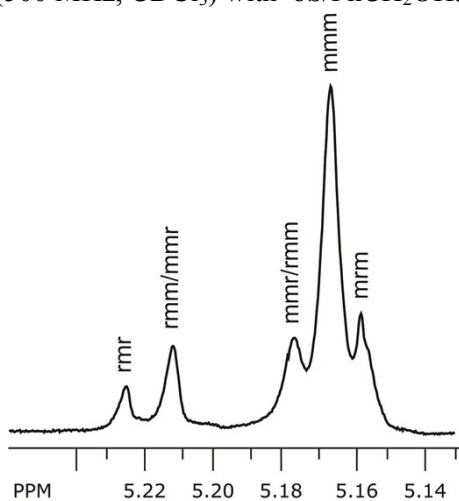


Fig. S44 Homonuclear decoupled ^1H NMR spectrum of the methine region of PLA prepared from *rac*-lactide at 70 °C in toluene (500 MHz, CDCl_3) with **7a**/ PhCH_2OH .

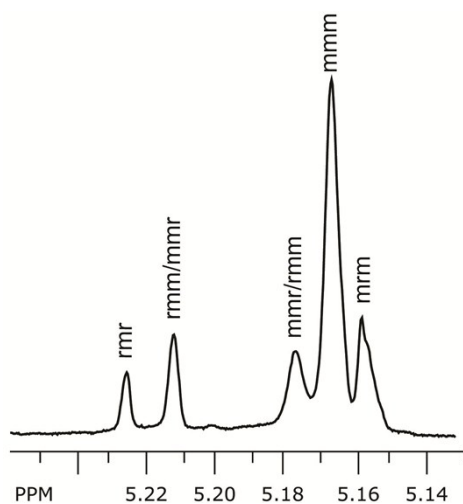


Fig. S45 Homonuclear decoupled ^1H NMR spectrum of the methine region of PLA prepared from *rac*-lactide at 70 °C in toluene (500 MHz, CDCl_3) with **7b**/PhCH₂OH.

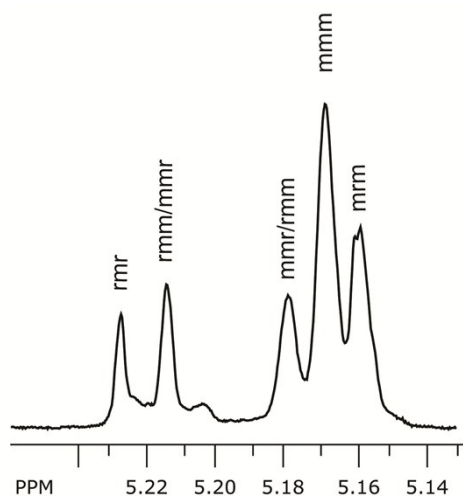


Fig. S46 Homonuclear decoupled ^1H NMR spectrum of the methine region of PLA prepared from *rac*-lactide at 70 °C in toluene (500 MHz, CDCl_3) with **8a**/PhCH₂OH.

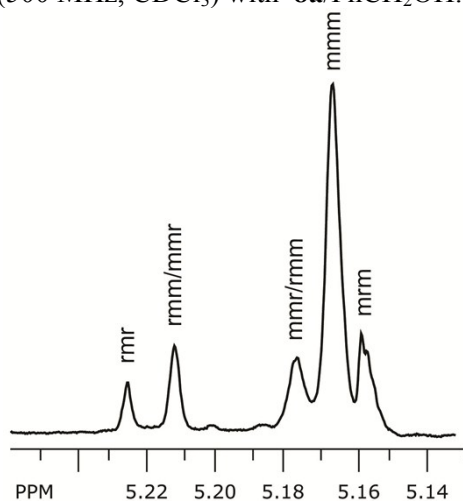


Fig. S47 Homonuclear decoupled ^1H NMR spectrum of the methine region of PLA prepared from *rac*-lactide at 70 °C in toluene (500 MHz, CDCl_3) with **8b**/PhCH₂OH.

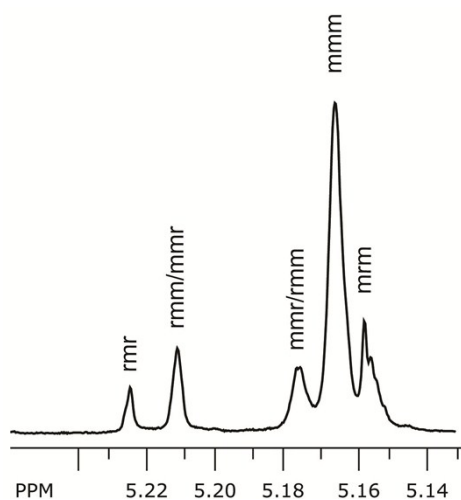


Fig. S48 Homonuclear decoupled ^1H NMR spectrum of the methine region of PLA prepared from *rac*-lactide at 70 °C in toluene (500 MHz, CDCl_3) with **9a**/ PhCH_2OH .

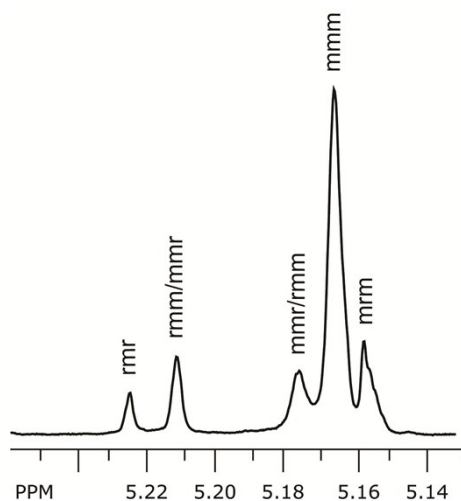


Fig. S49 Homonuclear decoupled ^1H NMR spectrum of the methine region of PLA prepared from *rac*-lactide at 70 °C in toluene (500 MHz, CDCl_3) with **9b**/ PhCH_2OH .

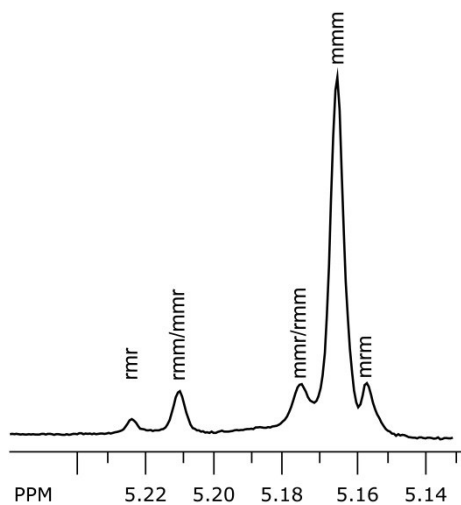


Fig. S50 Homonuclear decoupled ^1H NMR spectrum of the methine region of PLA prepared from *rac*-lactide at 50 °C in toluene (500 MHz, CDCl_3) with **4b**/ PhCH_2OH .

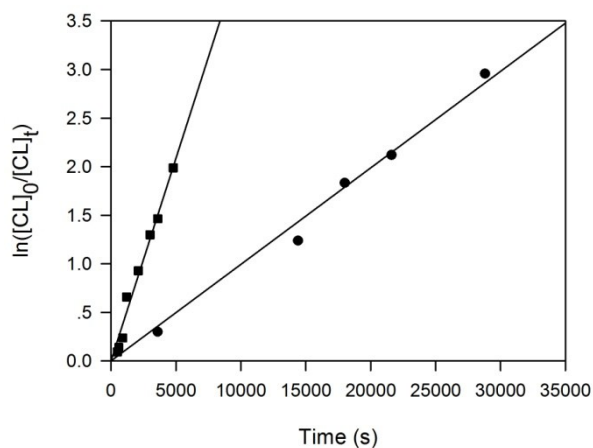


Fig. S51 Semilogarithmic plots of ε -CL conversion versus time in C_6D_6 at 40 °C with complexes **2a** (■) and **2b** (●) ($[\varepsilon\text{-CL}]_0/[\text{Al}] = 50$, $[\text{Al}]/[\text{PhCH}_2\text{OH}] = 1$, $[\varepsilon\text{-CL}]_0 = 0.83$ M, $[\text{Al}] = 16.67$ mM).

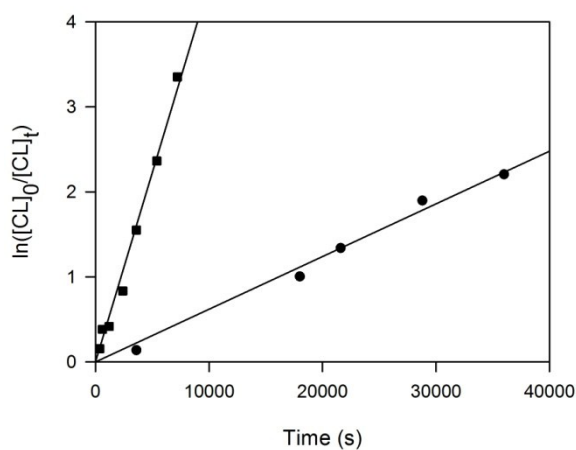


Fig. S52 Semilogarithmic plots of ε -CL conversion versus time in C_6D_6 at 40 °C with complexes **3a** (■) and **3b** (●) ($[\varepsilon\text{-CL}]_0/[\text{Al}] = 50$, $[\text{Al}]/[\text{PhCH}_2\text{OH}] = 1$, $[\varepsilon\text{-CL}]_0 = 0.83$ M, $[\text{Al}] = 16.67$ mM).

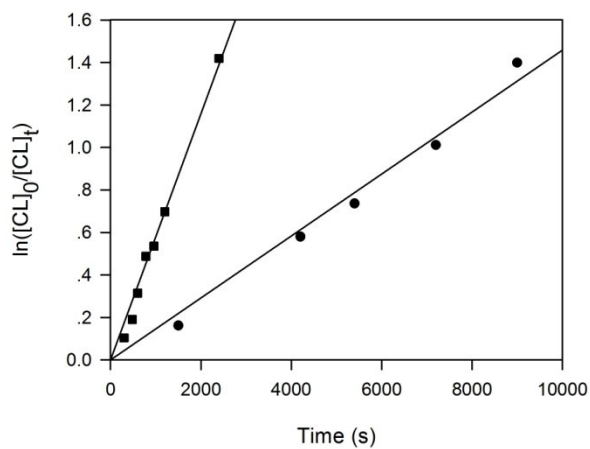


Fig. S53 Semilogarithmic plots of ε -CL conversion versus time in C_6D_6 at 40 °C with complexes **4a** (■) and **4b** (●) ($[\varepsilon\text{-CL}]_0/[\text{Al}] = 50$, $[\text{Al}]/[\text{PhCH}_2\text{OH}] = 1$, $[\varepsilon\text{-CL}]_0 = 0.83$ M, $[\text{Al}] = 16.67$ mM).

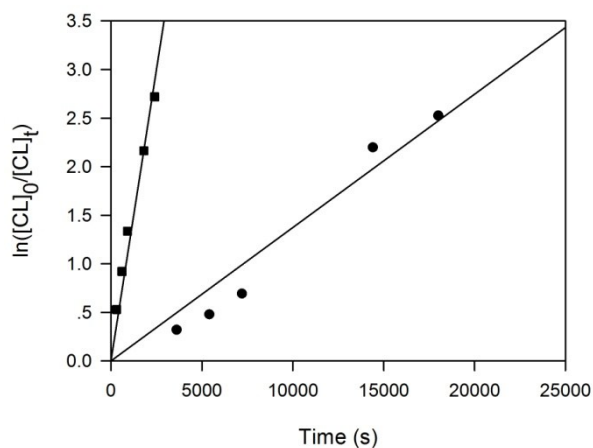


Fig. S54 Semilogarithmic plots of ε -CL conversion versus time in C_6D_6 at 40 °C with complexes **5a** (■) and **5b** (●) ($[\varepsilon\text{-CL}]_0/[\text{Al}] = 50$, $[\text{Al}]/[\text{PhCH}_2\text{OH}] = 1$, $[\varepsilon\text{-CL}]_0 = 0.83$ M, $[\text{Al}] = 16.67$ mM).

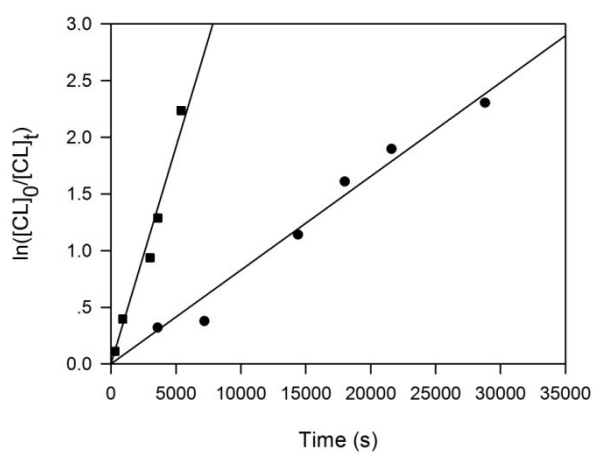


Fig. S55 Semilogarithmic plots of ε -CL conversion versus time in C_6D_6 at 40 °C with complexes **6a** (■) and **6b** (●) ($[\varepsilon\text{-CL}]_0/[\text{Al}] = 50$, $[\text{Al}]/[\text{PhCH}_2\text{OH}] = 1$, $[\varepsilon\text{-CL}]_0 = 0.83$ M, $[\text{Al}] = 16.67$ mM).

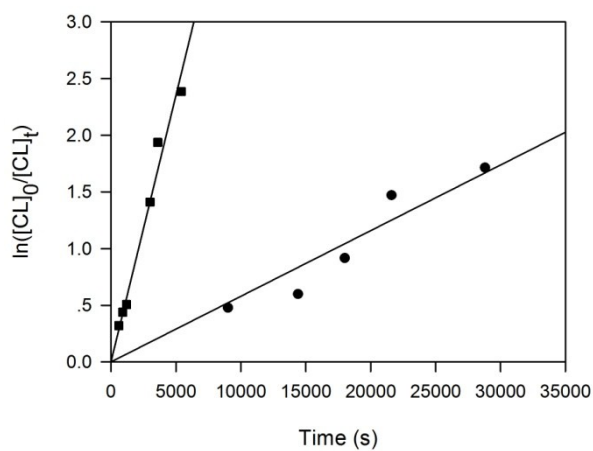


Fig. S56 Semilogarithmic plots of ε -CL conversion versus time in C_6D_6 at 40 °C with complexes **7a** (■) and **7b** (●) ($[\varepsilon\text{-CL}]_0/[\text{Al}] = 50$, $[\text{Al}]/[\text{PhCH}_2\text{OH}] = 1$, $[\varepsilon\text{-CL}]_0 = 0.83$ M, $[\text{Al}] = 16.67$ mM).

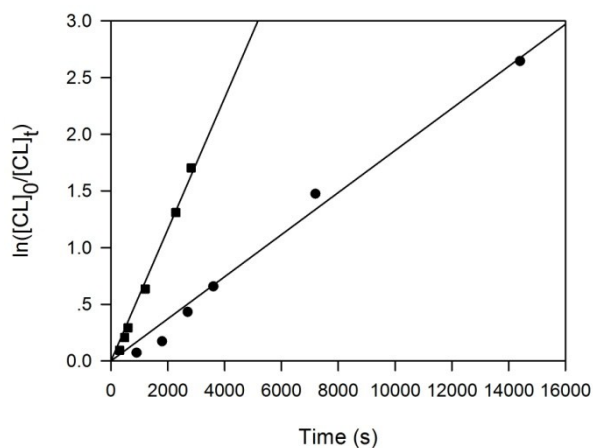


Fig. S57 Semilogarithmic plots of ϵ -CL conversion versus time in C_6D_6 at 40 °C with complexes **8a** (■) and **8b** (●) ($[\epsilon\text{-CL}]_0/[\text{Al}] = 50$, $[\text{Al}]/[\text{PhCH}_2\text{OH}] = 1$, $[\epsilon\text{-CL}]_0 = 0.83$ M, $[\text{Al}] = 16.67$ mM).

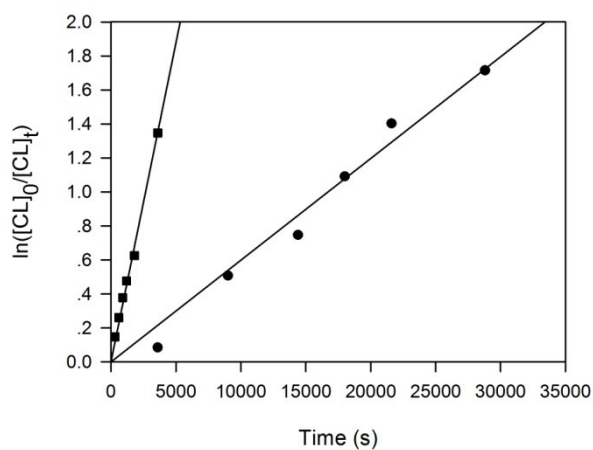


Fig. S58 Semilogarithmic plots of ϵ -CL conversion versus time in C_6D_6 at 40 °C with complexes **9a** (■) and **9b** (●) ($[\epsilon\text{-CL}]_0/[\text{Al}] = 50$, $[\text{Al}]/[\text{PhCH}_2\text{OH}] = 1$, $[\epsilon\text{-CL}]_0 = 0.83$ M, $[\text{Al}] = 16.67$ mM).

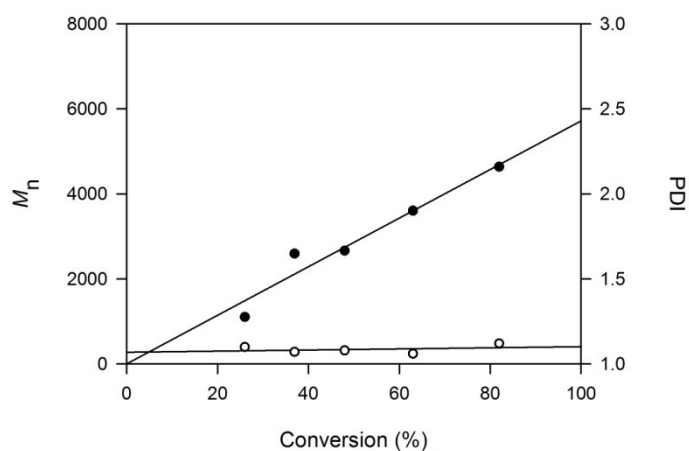


Fig. S59 Plot of PLA M_n (●) (versus polystyrene standards) and PDI (○) as a function of monomer conversion for a ϵ -CL polymerization using **1b**/PhCH₂OH ($[\epsilon\text{-CL}]_0/[\text{Al}] = 50$, C_6D_6 , 40 °C).